Influence of symmetry energy on fragment production

A dissertation submitted in the partial fulfilment of requirement for the award of the

Degree of

Masters of Science
In
Physics

Submitted by
RUBINA BANSAL
Roll no.-300904013
Under the esteemed guidance of
Dr. Suneel Kumar
(Assistant professor)
School of physics and material science
Thapar University
PATIALA (PUNJAB)-147004

June 2011.

Dedicated

To

My FAMILY

CERTIFICATE

This is to certify that the dissertation entitled ' Influence of symmetry energy on fragment production' submitted by Rubina Bansal (Roll no. 300904013) of M.Sc(physics), Thapar University, Patiala, was carried out by her under my supervision. This work has not submitted this material for credit towards any other degree at Thapar University, Patiala or any other University.

S Kumar
14/7/20

Dr.Suneel Kumar
Assistant Professor
School of Material Science and Physics,
Thapar University,
Patiala.

tersigned by:

.P. Pandey
. & Head)
ol of physics and Material Science,
ar University,
la.

Dr. S.K. Mohapatra
Dean of academic Affairs
Thapar University,
Patiala.

ACKNOWLEDGEMENT

I owe my deepest gratitude to **Dr. Suneel Kumar**, *my supervisor*, who has been an inspiration during my work. Without him, thi would not have been possible. I thank him for his patience and encourageme carried me on through difficult times, and for his insights and suggestio helped to shape my skills. I express my sincere thanks to him for his v guidance in carrying out work under his effective supervision, encourageme cooperation. His visionary thoughts have influenced me greatly. His dy attitude has empowered me with zeal of energy to conquer the minor detail research work.

I also thank **Dr. O. P. Pandey**, Professor and Head, School of Phy Materials Science for his support and providing facilities. Special thanks are d my friends and the staffs specially PhDs scholar **Anupriya Jain** and **Kara Vinayak** at the School of Physics and Material Sciences for providing me a atmosphere and encouraging me throughout this work.

I am deeply thankful to my Family their moral support and patience ha fruit through completion of this report.

Rubina

(**Rubina Bansal**)

Roll No. 300904013

Date: 14-7-2k11

Place: Thapar University,

Patiala.

ABSTRACT

The present work deals with the theoretical study dealing with influence of density dependence of symmetry energy on multifragmentation and in heavy ion collision at intermediate energies. We present a complete systematic theoretical study of multifragmentation for mass symmetric colliding nuclei for heavy-ion reactions in the energy range between 50 MeV/nucleon and 1000 MeV/nucleon by using soft equations of state using isospin dependent quantum molecular dynamics (IQMD) model. We envision an interesting outcome for symmetric colliding nuclei small but clear signature influence of density dependence of symmetry energy on fragmentation can be seen. The effect of isospin dependent and constant cross section also has been studied.

TABLE OF CONTENTS

Chapter 1 – Introduction

Chapter 2 – Methodology

List of figures

CHAPTER 1

Introduction

1.1 Influence of nuclear physics

The science of nuclear physics deals with the properties of nuclear matter which makes up the massive centre of the atom. The main interest revolves around the structure of nucleus. The term heavy ion is generally used for nuclei which are heavier than the helium nucleus. A heavy ion can be singly ionized or can have any intermediate charge state. A classical picture of heavy ion collision might be possible [1]. When two nuclei collide at energy less than 10 MeV/nucleon then fission take place. When energy is less than 50 MeV/nucleon then spallation takes place. When energy is between 100-600 MeV/nucleon then multifragmentation take place. When two heavy nuclei collide at high energy, they create strongly interacting matter at energy densities far above that of normal nuclei. This has been the route for creating new phases of matter composed of quarks and gluons for almost a decade at relativistic heavy ion collider (RHIC).

A diagram that depicts existence of different phases of a system under equilibrium is termed as phase diagram. The schematic phase diagram of hot dense nuclear matter is as shown in figure 1.1. Here normal density is represented along X-axis and temperature is represented along Y-axis. The Liquid-gas phase (LGP) transition region at the lower left corner at temperature below 15 MeV and density is less than normal density [2]. At very high temperatures the hadrons melt and their constituents, the quarks and gluons, form a new phase of matter, the so called quark-gluon plasma i.e. region of very high density and temperature corresponds to Quark-Gluon Plasma phase (QGP) [3]. At intermediate temperature and density Hadron Matter phase (HM) exists. As the temperature and the density are raised, the nucleons are excited into "baryon resonances" which subsequently decay into pions and nucleons. This mixture of nucleons, baryonic resonances and mesons is called Hadronic Matter. The neutron star (NS) density region extends from the low density upto more than 10 times the normal nuclear matter density. The typical temperature is less than 10 MeV

for newly born neutron star and less than 0.01 MeV for cold stars. In highly compressed cold nuclear matter as it may exist in the interior of neutron stars - the baryons also lose their identity and dissolve into quarks and gluons. The two transition region or/and phase co-existence separates the QGP phase from HM phase [4]. A critical point separates the two regions. The chemical freeze out point reached at RHIC and LHC experiments. The "deconfinement" phase transition from hadronic matter to quark-gluon matter takes place at a temperature of about 170 MeV (at net baryon density zero) which is 130 thousand times hotter than the interior of the sun. Such conditions did exist in the early universe, a few microseconds after the big bang and can be created in heavy ion collisions at ultra-relativistic energies such that QGP and HM phase existed in the early stage of the evolution of universe are inaccessible today.

Current investigations of the phase diagram suggest a strong dependence of the properties of the transition on the baryon number density. While the transition is a smooth crossover at low density it is expected to be first order at high density. The two regions are separated by a second order transition point (critical point). At the "critical point" the deconfinement/chiral phase transition is predicted to change its character. The highest net baryon densities are expected for nuclear collisions in the beam energy range between 10 and 40 GeV/c.

The region of very high temperature and density corresponds to quark gluon plasma phase (QGP) but under ordinary conditions neither quarks nor gluons are ever free. The farther apart they get, the stronger the force between them. Because mass and energy are interchangeable, as described by Einstein's $E=Mc^2$, eventually the energy that would be needed to separate them goes into creating new bound quarks instead.

The phase diagram of strongly interacting particle matter as function of temperature and baryon number density is studied theoretically in lattice calculations as well as experimentally in heavy ion collision experiments at Brookhaven, USA (RHIC) and future European accelerators at CERN, Geneva (LHC) and the GSI in Darmstadt. RHIC was designed to collide heavy nuclei (as heavy as gold, whose nucleus consists of 79 protons and 118 neutrons) at energies so high that during the near light speed

collisions, conditions cease to be anything like ordinary. Dense, hot fireballs blossom in the collisions, forming a plasma in which neither quarks nor gluons are bound together, instead they move independently with almost complete freedom.

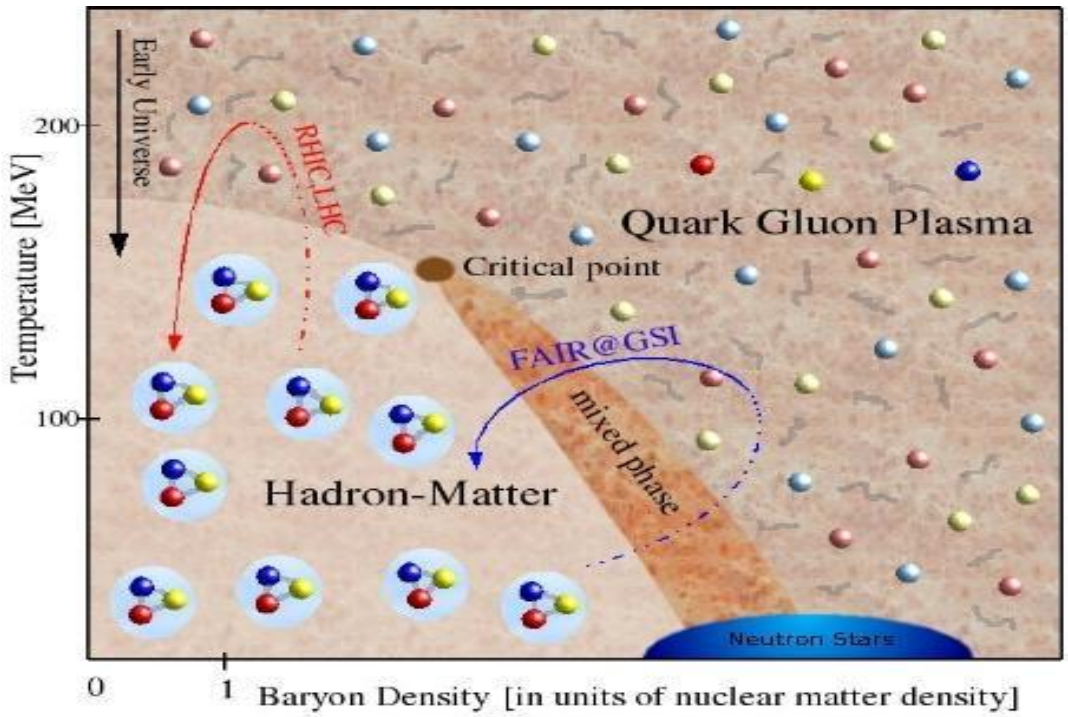

Fig.1.1: Schematic phase diagram for the hot dense matter.

The nuclear structure studies have provided vital information about the nuclear interaction fusion-fission, cluster radio activities as well as halo nuclei [3]. The heavy-ion reaction during which the matter undergoes through compression and expansion stages are true testing grounds for the hot and dense nuclear matter.

1.2 Symmetry energy

Symmetry energy is that energy at which protons in the nucleus tends to be neutrons and vice-versa. The symmetry energy *E*sym (*ρ*) of nuclear matter characterizes how the energy rises as one moves away from equal numbers of neutrons and protons. Nuclear symmetry energy *E*sym(*ρ*), which encodes the energy related to neutron-proton asymmetry in the equation of state of nuclear matter, is a fundamental quantity currently under intense investigation in both nuclear physics and astrophysics. Both the magnitude and density dependence of *E*sym (*ρ*) are critical for understanding

not only the structure of rare isotopes and the reaction mechanism of heavy-ion collisions but also many interesting issues in astrophysics, such as the structure and composition of neutron stars. Despite much effort made both experimentally and theoretically, our current knowledge about *E*sym (ρ) is still poor.

1.2.1 Density dependence of the symmetry energy

Various interaction used in *ab initio* microscopic calculations predict different forms of the nuclear equation of state above and below the normal nuclear matter density, and away from the symmetric nuclear matter[4]. In general two different type of the density dependence of the symmetry energy have been predicted. One, where the symmetry energy increases monotonically with increasing density ("stiff" dependence) and the other, where the symmetry energy increases initially up to normal nuclear density and then decreases at higher densities ("soft" dependence). Constraining the form of the density dependence of the symmetry energy is important not only for a better understanding of the nucleon-nucleon interaction, and hence its extrapolation to the structure of neutron-rich nuclei [5], but also for determining the structure of compact stellar objects such as neutron stars.

By studying the isotopic yield distribution of fragments obtained by multifragmentation one can extract important information about the symmetry energy and its density dependence. It has been shown from experimental measurements that the ratio of the fragment yields, R_{21}(N,Z), taken from two different multifragmentation reactions, 1 and 2, obeys an exponential dependence on the neutron number (N) and the proton number (Z) of the fragments; an observation known as isoscaling [6]. The dependence is characterized by the relation

$$R_{21}(\mathrm{N,Z}) = Y_2(N,Z)/Y_1(N,Z) = Ce^{(\alpha N+\beta Z)} \quad (1)$$

Where Y_2 and Y_1 are the fragment yields from the neutron-rich and the neutron-deficient systems, respectively. C is an overall normalization factor, and α and β are the parameters characterizing the isoscaling behaviour. Isoscaling is also theoretically predicted by the dynamical [7, 8] and statistical [9, 10] models of multifragmentation. The various combinations of target and projectile nuclei allowed for a range of N/Z (neutron-to-proton ratio) (1.04–1.23) of the system to be studied, while keeping the

total mass constant (A = 98). From various theoretical independent studies the parameterized form of the density dependence of the symmetry energy obtained, which are as

Reference	Parametrization	Studies
Fuchs et al.	$32.9(\rho/\rho o)^{0.59}$	relativistic Dirac-Brueckner calculation
Heiselberg et al.	$32.0(\rho)^{0.60}$	Variational calculation
Danielewicz et al.	$31(33)(\rho/\rho o)^{0.55(0.79)}$	BE, skin, isospin analog states
Tsang et al.	$12.125(\rho/\rho o)^{2}$	Isospin diffusion
Chen et al.	$31.6(\rho/\rho o)^{1.05}$	Isospin diffusion
Li et al.	$31.6(\rho/\rho o)^{0.69}$	Isospin diffusion
Piekarewicz et al.	$32.7(\rho/\rho o)^{0.64}$	Giant resonances
Shetty et al.	$31.6(\rho/\rho o)^{0.69}$	Isotopic distribution
Famiano et al.	$32.0(\rho/\rho o)^{0.55}$	neutron-proton emission ratio
Tsang et al.	$23.4(\rho/\rho o)^{0.6}$	Isotopic distribution

The best estimate of the density dependence of the symmetry energy can be parameterized as

$$C_{\mathrm{sym}}(\rho) = C^{o}_{\mathrm{sym}} \left(\frac{\rho}{\rho_o} \right)^{\gamma} (\mathrm{MeV}) \tag{2}$$

where C^{o}_{sym}, is the value of the symmetry energy at normal density and γ is the parameter that characterizes the stiffness of the symmetry energy, the above dependences used by Chen *et al.* can be written as $E\mathrm{sym} \approx 31.6\ (\rho/\rho^{0})^{\gamma}$, where, γ = 1.6, 1.05, and 0.69, respectively. Figure 1.2 shows various forms of the density dependence of the symmetry energy in isospin asymmetric nuclear matter used by Chen *et al.* [11], and those used in the present dynamical model analysis. The dashed curves correspond to the momentum dependent Gogny interactions used by Chen *et al.* to explain the NSCL-MSU isospin diffusion data. It was shown that the experimental data agrees better with the choice of Gogny-AS interaction.

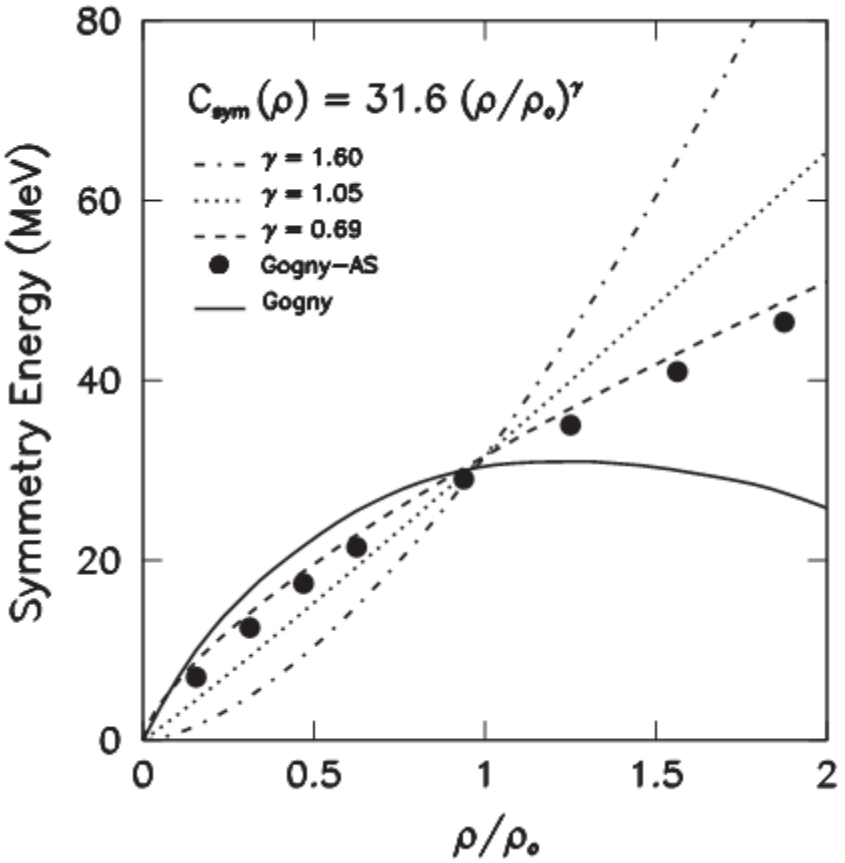

Fig.1.2. Different forms of the density dependence of the nuclear symmetry energy used in the dynamical analysis of the present measurements on isoscaling data and the isospin diffusion measurements of NSCL-MSU [11].

By parameterizing the density dependence of the symmetry energy that explains the present isoscaling data, one obtains, $C_{sym}(\rho) \approx 31.6\ (\rho/\rho^0)^\gamma$,where γ = 0.69, from the dynamical model analysis. This form of the density dependence of the symmetry energy is consistent with the parameterization adopted by Heiselberg and Hjorth-jensen in their studies on neutron stars [12].Numerous many-body calculation [13] and empirical liquid drop mass formula [14] predict symmetry energy near normal density to be around 30 MeV, but direct experimental determination does not exist.

1.2.2 Excitation energy dependence of symmetry energy of finite nuclei

The symmetry energy is used in the local density approximation to evaluate the excitation energy dependence of the symmetry energy coefficient of finite nuclei in a micro canonical formulation that accounts for thermal and expansion effects. A nucleus expands with excitation with increasing temperature in general. This implies an excitation energy dependence of the symmetry energy because of the

density change. Experimentally, this information is generally extracted [4] from the fit of the experimental isotopic distributions at different excitation energies to those obtained from a model for multifragmentation like the statistical multifragmentation model (SMM) [15] or from isoscaling [16]. Currently, calculations for the energy dependence of the symmetry energy are available for infinite matter, but no microscopic calculation has yet been performed for the energy dependence of finite nuclei.

1.3 Experimental review of symmetry energy on multifragments

Experimentally, the symmetry energy is not a directly measurable quantity and has to be extracted indirectly from observables that are related to the symmetry energy. The experimental determination of the symmetry energy is therefore dependent on how reliable the model that describes the experimental observable.

Experimental determination of the symmetry energy is based on two methods

1) In which the density dependence of the symmetry energy is assumed in the theoretical calculation and the experimental observable reproduced using the dependence that best explains the data.
2) Other method in which density dependence of the symmetry energy is not known priori and the symmetry energy is studied by mapping its value at each density.

In 1980's, Jakobsson et.al. [18], observed the multiple emission of IMF's in the emulsion irradiated by the carbon beam of 250 MeV/nucleon. This result created the interest of the nuclear community toward multifragmentation. Warwick et.al.[19] found that multifragmentation is a dominant reaction channel at beam energies higher than 35 MeV/nucleon. Further, the Purdue group [20] conjectured that multifragmentation is a clear signature for the phase transition between a gaseous and liquid phase of nuclear matter, which occurs around a density of $0.4\rho_0$; ρ_0 is the normal nuclear matter density. Since then, the study of multifragmentation has been considered of great interest. Lots of detectors included the forward and 4π designed to understand the each and every aspect in detail.

First accelerator in this series was the BEVALAC accelerator at Lawrence Berkeley Laboratory that led way to high energy accelerators built at the Michigan state university (MSU)(USA). With the passage of time, the Grand Accelerateur National D'ions Lourds (GANIL)(France), Relativistic Heavy-Ion Collider (RHIC) (USA),

Superconducting Super-Collider (SSC) at BNL (USA), NSF-Arizon accelerator at the university of Arizona (USA), Vivitron Accelerator in Strasbourg (France), Superconducting Cyclotron (SC) at Texas (USA), Superconducting Cyclotron (SC) and CHIMARA detector at Laboratori Nazionali del Sud in INFN, Catania (Italy) and Heavy-ion Synchrotron SIS accelerator at GSI (Germany) etc. has contributed lot in the field of multifragmentation.

The Emulsion experiment [18, 21] was among the first attempts to study the multifragmentation. They provided a unique possibility to study the fusion, multifragmentation as well as vaporization at intermediate energies. Through the process of multifragmentation, critical exponents like surface energy, volume energy, symmetry energy, entropy etc. [22] are extracted for the asymmetric reactions in the energy region of 1 GeV/nucleon. In the earlier studies, similar exponents were extracted for symmetric Au + Au collisions [23].

The symmetric collisions are studied by the Superconducting Cyclotron of the Laboratory Nationali del Sud of INFN (Italy). They considered the reactions of Nb + Nb (at 17, 23, 30 and 38 MeV/nucleon) and Sn + Sn (at 29.6, 38 MeV/nucleon) [24]. The multiplicity of LCP's and IMF's in peripheral and semi-peripheral collisions as a function of excitation energy of emitting source, mass of the system and beam energy have been presented [24]. The difference in isotropic composition of fragments emitted from statistical and dynamical production process [25, 26] has also been observed.

The FOPI and ALADIN groups at GSI studied the multifragmentation process over a wide range of masses from C to Pb with incident energies ranging from 100 to 1000 MeV/nucleon [27]. A rise and fall in the multifragmentation is also reported by ALADIN collaboration for the reaction of Au+Au [27]. In the first experiment, S031 (July 1990), the fragmentation of Au- projectiles was investigated at 600 MeV/nucleon. The second experiment, S022 (October 1991), was performed in collaboration with the MINIBALL/WALL groups from Michigan State University and Washington University, using Au beams with energies of 100, 250, 400 and 600 MeV/nucleon. The main emphasis in this experiment was a full coverage of all fragments produced in the interaction. Moreover, the fragment multiplicities and correlations are found to obey the universal behaviour [27]. INDRA group at GANIL (France) is also one of the leading

groups in this field. They analyze a variety of parameters in multifragmentation. The system size effects, the role of system size in entrance channel as well as Coulomb instabilities, kinetic energy spectra and fragment velocity correlation are studied in nearly asymmetric reactions. They study symmetric reaction of $^{197}Au_{79}$ + $^{197}Au_{79}$ at 40 and 150 MeV/nucleon [28]. It is also observed that mutifragmentation is responsible for fragment production around the excitation energy of 3 MeV/nucleon [29].

1.4 Theoretical review of symmetry energy on multifragments

Theoretically, the symmetry energy can be determined from microscopic calculations such as the Brueckner-Hartree-Fock (BHF) and the Dirac-Brueckner-Hartree-Fock (DBHF) calculations, or the phenomenological calculations such as the Skyrme Hartree-Fock (SHF) and the relativistic mean field (RMF) calculations [17]. These calculations currently predict wide range of symmetry energies for densities below and above normal nuclear density, ρ^O = 0.16 fm^{-3}. A native picture of nuclear reactions at intermediate energies undergoes three important steps:

1. Initial stage where the target and projectile are boosted toward each other with proper centre of mass energy.
2. Compression and expansion stage,
3. Pre-fragment source is formed and reaches equilibrium; a secondary decay process of various emitted fragments.

The theoretical models for the processes at intermediate energies can be divided into two categories: Statistical and Dynamical model.

1.4.1 Statistical model

Statistical models include multiparticle phase space models, such as the Statistical Multifragmentation Model (SMM) [30, 31] and the Berlin Multifragmentation Model [32], which can incorporate specific nuclear properties directly. Accordingly, a semi micro canonical version of SMM [31] that incorporates detailed nuclear structure information relevant to the population and secondary decay of the excited fragments was developed [33]. Additional static models include Percolation [34], Lattice Gas Approach [35] and Expanding Emitting Source (EES) model [36]. These approaches have the virtue of providing relatively simple schematic algorithms suitable for the exploration of critical phenomena in finite systems. The limitation of the statistical models is:

(i) The situation at the start of reaction is based on some assumption for the degree of thermalization [31].

(ii) The statistical models give a better description only of the later/final stage of the reaction.

Our aim is to study all the stages discussed earlier which are initialization, compression and expansion. Hence the statistical models are neglected in this study. This study is possible by the dynamical models only.

1.4.2 Dynamical model

The dynamical approaches such as the Time Dependent Hartree Fock (TDHF) [37] or its semi-classical version called Vlasov equation (in phase space) [39] are suitable at low incident energies where nucleon-nucleon collisions are negligible. However, a suitable and reasonable approach for the intermediate energy heavy-ion physics should treat the nucleon-nucleon scattering and mean field on equal footing. Some attempts were made in the literature to extend the TDHF theory to take care of the residual n-n interactions, which are responsible for the two-body collisions. This was dubbed as Extended Time dependent Hartree-Fock (ETDHF) theory [39].

In the first attempt, semi-classical version of ETDHF theory i.e. Vlasov equation [38] was coupled with nucleon-nucleon collisions and thus, a new realization, named as Boltzmann-Uehling-Uhlenback equation (BUU), was developed to study the large deviation problems of low, intermediate and relativistic heavy-ion collisions. . The semi-classical models include mainly the two types: the BUU and the QMD model. In BUU, N parallel runs communicate with each other, therefore, event by event correlation cannot be analyzed. However, Bonasara et.al. [40], solved the collision integral using the concept of mean free path. In this method, N parallel runs do not communicate with each other, event by event correlations are preserved. At intermediate energy region, we opt those methods where correlations and fluctuations among nucleon can be preserved.

The Classical Molecular Dynamics (CMD) [41] approach (or the equation of motion), in principle, is capable of predicting the fragments production. It also incorporates the complete classical N-body dynamics which is necessary to describe the formation of the fragments. The quantum features play a very important role at low

incident energies. The above approach was later extended to incorporate the quantum features by Aichelin and Stocker [37, 42]. This new approach, which explicitly incorporates the N-body correlations as well as nuclear matter equation of state and important quantum features (like the Pauli principle, Stochastic scattering and particle production), was dubbed as Quantum Molecular Dynamics (QMD) model [37] explain in 2.4. Semi-classical transport model such as IBUU [43], SMF [45] and IQMD [46] have been successfully developed in recent years to describe nuclear reactions induced by neutron-rich nuclei at intermediate energies. The isospin dependent Boltzmann-Uehling-Uhlenback (IBUU) transport model was included in the dynamics through nucleon-nucleon collisions by using isospin dependent cross-sections and Pauli blocking factors, the symmetry potential $V_{sym}(\rho, \delta)$, and the coulomb potential. This model was used to calculate the ratio of yield of neutron and protons in pre-equilibrium emission [44]. Accurate solution of the BUU equation average away fluctuations in the density that might lead to the formation of fragments in an individual collision. The density fluctuations that lead to the fragment production are suppressed in the BUU equation, so the calculation of fragment yield directly via BUU model is not feasible. Therefore, alternate model such as, Stochastic Mean Field (SMF) model [45] and Isospin Quantum Molecular Dynamics (IQMD) model [46] has been developed to address the density fluctuations. The SMF, like IBUU, describes the time evolution of the collision using self-consistent mean field.

Dynamical models identify the two nucleons in the same fragment if their centroids are less than some distance [47]. This method is known as Minimum Spanning Tree (MST) method. Till today, it is one of the most extensively used methods. Several refinements to this method have been proposed including momentum cut and binding energy cut [48]. One more and newly developed secondary model is Simulated Annealing Clusterization Algorithm, developed by Puri, Hartnack and Aichelin [49], which is based on the minimization of energy of the system. We shall study the phenomena of multifragmentation using IQMD model.

1.5 Different phenomena at intermediate energies

1.5.1 Multifragmentation

The initial information for calculation of multifragmentation stage consists from the atomic mass number A, charge Z of excited nucleus and its excitation energy U. At high excitation energies U/A > 3 MeV the multifragmentation mechanism, when nuclear system can eventually breaks down into fragments, becomes the dominant. Later on the excited primary fragments propagate independently in the mutual Coulomb field and undergo de-excitation. At comparatively low excitation energy (temperature) the produced system is known as compound nucleus, and system will disintegrate into a small number of fragments M ≤ 4 and number of channel is not huge. For such situation a direct (microcanonical) sorting of all decay channels can be performed the configuration of two colliding nuclei before collision and after collision with energy deposited in the central region as shown in Fig. 1.3.

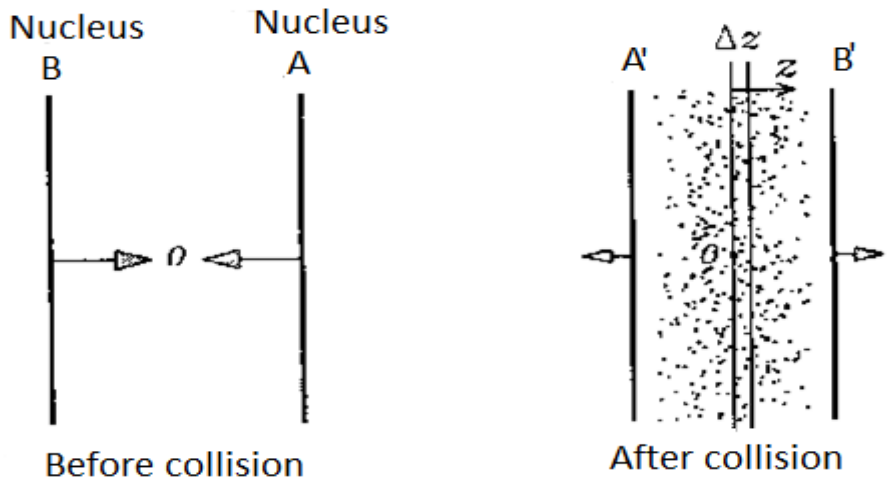

Fig. 1.3: The configuration of two colliding nuclei before collision and after collision.

1.5.2 Collective flow

"The transverse motion imparted to the particles during the collision of two nuclei is known as collective flow." The determination of the equation of state (EOS), the relationship between pressure and volume for nuclear matter, is an important objective of nuclear physics. Information about the equation of state can be extracted from the collective flow of nuclear matter deflected sidewards from the hot and dense region formed by the overlap of projectile and target nuclei Fig.1.4 shows the nuclear matter distributions for the projectile and target nuclei before the collision (on

the left) and a sidewards deflection of the nuclear matter after the collision (on the right) which is frequently termed "sidewards collective flow". This flow reflects the interplay of collective and random motions. For a thermalized system, the random motions of emitted fragments are dictated by the thermal energy, which is independent of mass.

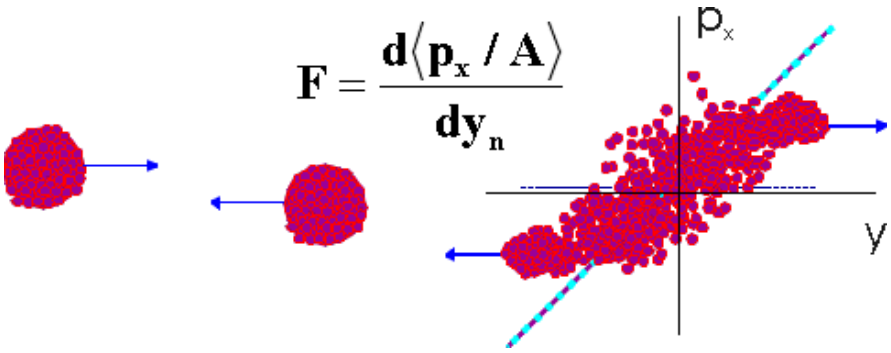

Fig. 1.4: shows the nuclear matter distributions in x-direction with respect to y direction.

1.5.3 Isospin Physics

Isospin is a physical quantity which is mathematically analogous to spin. Isospin was introduced by Werner Heisenberg to explain the fact that the strength of the strong interaction is almost the same between two protons or two neutrons as between a proton and a neutron, unlike the electromagnetic interaction which depends on the electric charge. In this review, we discuss recent theoretical studies of the equation of state of isospin asymmetric nuclear matter and its relations to the properties of neutron stars and radioactive nuclei. The in-medium nucleon-nucleon cross sections at different isospin states are reviewed as they affect significantly the dynamics of heavy ion collisions induced by radioactive beams. The study of nuclear stopping in terms of isospin equilibration, the dependence of nuclear collective flow and balance energy on the isospin-dependent nuclear equation of state and cross sections, the isospin dependence of total nuclear reaction cross sections, and the role of isospin in pre-equilibrium nucleon emissions and sub-threshold pion production.

1.6 Organization of thesis

The thesis is organized as follows:

In chapter 2, we will describe various theoretical models in brief. The primary models, Quantum Molecular Dynamics (QMD) and Isospin-dependent Quantum Molecular Dynamics (IQMD) will be discussed in detail.

In chapter 3, we shall study the time evolution and incident energy on the production of different kind of fragments like free particles, light mass fragments (LMF's), medium mass fragments (MMF's) and Intermediate mass fragments(IMF's), with three different type of cross-section eg. Constant, isospin dependent and isospin independent, using IQMD model in collision of Au + Au, Xe + Xe, Zr + Zr, Ca + Ca, Ne + Ne nuclei. The reactions are analyzed with MST method.

1.7 REFERENCES

[1] D.C. Tayal Nuclear Physics.

[2] H. Muller and B.D. Serot, Phys. Rev. **C 52**, 2072 (1995) .

[3] L.C. Vaz, J.M. Alexander and G.R. Satchler, Phys. Rep. **69**, 373 1981; M. Beckerman, Rep. Prog . Phys. **51**, 1047 (1988).

[4] D.V. Shetty, S.J. Yennello, G.A. Souliotis, Phys.Rev. **C 76**.024606 (2007)

[5] B. A. Brown, Phys. Rev. Lett. **85**, 5296 (2000).

[6] M. B. Tsang, W. A. Friedman, C. K. Gelbke, W. G. Lynch, G. Verde, and H. S. Xu, Phys. Rev. Lett **86**, 5023 (2001).

[7] A. Ono, P. Danielewicz, W. A. Friedman, W. G. Lynch, and M. B. Tsang, Phys. Rev. **C 68**, 051601(R) (2003).

[8] Q.Li, Z. Li, andH. Stocker, Phys.Rev.**C 73**, 051601(R) (2006).

[9] A. S. Botvina, O. V. Lozhkin, andW. Trautmann, Phys. Rev. **C 65**, 044610 (2002).

[10] Al. H. Raduta and Ad. R. Raduta, Phys. Rev. **C 65**, 054610 (2002).

[11] L.W.Chen, C.M. Ko, andB. A. Li,Phys. Rev. Lett. **94**, 032701 (2005).

[12] H.Heiselberg and M. Hjorth-jensen,Phys. Rep.**328**, 237 (2000).

[13] J.M. Pearson and R.C. Nayak, Nucl. Phys. **A 668**, 163 (2000).

[14] W. Myers and W. Swiatecki, Nucl. Phys. **81**, 1 (1966)

[15] J. P. Bondorf *et al.*, Phys. Rep. **257**, 133 (1995).

[16] A. Ono, P. Danielewicz, W. A. Friedman, W. G. Lynch, and M. B. Tsang, Phys. Rev. **C 68**, 051601(R) (2003).

[17] B.A. Li, L.W. Chen, and C.M. Ko, Phys. Rep. **464**, 113 (2008).

[18] B. Jakobsson et al., Z. Phys. **A 307**, 293 (1982).

[19] A. I. Warwick et al., Phys. Rev. **C 27**, 1083 (1983).

[20] J. E. Finn et al., Phys. Rev. Lett. **49**, 1321 (1982).

[21] S. R. Souza et al., Phys. Rev. **C 50**, 257 (1994).

[22] N. T. Porlie, Nucl. Phys. **A 681**, 253 (2001); B. K. Srivastva et al., Phys. Rev. **C 65**, 054617 (2002); J. B. Elliott et al., Phys. Rev. **C 71**, 024607 (2005); L. G. Moretto, C O. Dorso, J. B. Elliott, and L. Phair, Phys. Rev. **C 77**, 037603 (2008).

[23] A. Insolia et al., Phys. Rev. **C 61**, 044902 (2000).

[24] S. Piantelli et al., Phys. Rev. **C 74**, 034609 (2006); S. Piantelli et al., Phys. Rev. **C 78**, 064605 (2008).

[25] P. M. Milazzo et al., Phys. Lett. **B 509**, 204 (2001).

[26] P. M. Milazzo et al., Nucl. Phys. **A 703**, 466 (2002).

[27] C. A. Ogilvie et al., Phys. Rev. Lett. **67**, 1214 (1991); J. Hubele et al., Phys. Rev. **C 46**, R1577 (1992); M. Begemann-Blaich et al., Phys. Rev. **C 48**, 610 (1993); G. F. Peaslee et al., Phys. Rev. **C 49**, R2271 (1994); A. S. Botvina et al., Nucl. Phys. **A 584**, 737 (1995); A. Schuttauf et al., Nucl. Phys. **A 607**, 457 (1996); N. T. B. Stone et al., Phys. Rev. Lett. **78**, 2084 (1997); A. S. Botvina et al., Phys. Rev. **C 74**, 044609 (2006).

[28] J. Lukasik et al., Phys. Rev. **C 66**, 064606 (2002).

[29] L. Manduci et al., Nucl. Phys. **A 811**, 93 (2008).

[30] J. P. Bondorf, A.S. Botvina, A.S. Iljinov, I.N. Mishustin, and K. Sneppen, Phys. Rep. **257**, 133 (1995). S. Pal, S. K. Samaddar, and J. N. De, Nucl. Phys. **A 608**, 49 (1996), D. K. Srivastava et al., Nucl-th/0506075 (2005); L. Satpathy, M. Mishra, A. Das, M. Satpathy, Phys. Lett. **B 237**, 181 (1990); C. B. Das, A. Das, L. Satpathy, M. Satpathy, Phys. Rev. **C 53**, 1833 (1996).

[31] J. P. Bondorf, R.Donangelo, I.N. Mishustin, C.J. Pethick, H. Schulz, and K. Sneppen, Nucl. Phys. **A 443**, 321 (1985); ibid **444**, 460 (1985); ibid **448**, 753 (1986). G. A. Souliotis et al., Phys. Rev. **C 75**, 011601 (2007); S. Pal, S. K. Samaddar, J. N. de, and B. Djerroud, Phys. Rev. **C 57**, 3246 (1998); A. Das, M. Mishra, M. Satpathy, and L. Satpathy, J. Phys. G: Nucl. and Part. **19**, 319 (1993).

[32] D. H. E. Gross, Rep. Prog. Phys. **53**, 605 (1990).

[33] S.R. Souza, W.P. Tan, R. Donangelo, C.K. Gelbke, W.G. Lynch, and M.B. Tsang, Phys. Rev. **C 62**, 064607 (2000).

[34] W. Bauer, D. R. Dean, U. Mosel, and U. Post, Phys. Lett. **B 150**, 53 (1985); W. Bauer, U. Post, D. R. Dean, and U. Mosel, Nucl. Phys. **A 452**, 699 (1986).

[35] J. Pan, S. Das Gupta, Phys. Lett. **B 344**, 29 (1995); J. Pan, S. D. Gupta, Phys. Rev. **C 51**, 1384 (1995); S. D. Gupta and J. Pan, Phys. Rev. **C 53**, 1319 (1996).

[36] W.A. Friedman, Phys. Rev. **C 42**, 667 (1990).

[37] H. Stocker and W. Greiner, Phys. Rep. **137**, 277 (1986); J. Aichelin, Phys. Rep. **202**, 233 (1991).

[38] G. F. Bertsch, H. Kruse and S. D. Gupta, Phys. Rev. C 29, R673 (1984); J. J. Molitoris, H H.Stocker, and B. L. Winer, Phys. Rev. **C 36**, 220 (1987); C. Gale et al., Phys. Rev. **C 41**, 1545 (1990); W. Cassing, W. Metag, U. Mosel, and K. Nitta, Phys. Rep. **188**, 363 (1990).

[39] E. Suraud, C. Gregoire, and B. Tamain, Prog. Part. Nucl. Phys. **23**, 357 (1989).

[40] A. Bonasera, G. F. Burgio, and M. D. Toro, Phys. Lett. **B 221**, 233 (1989); A. Bonasera, G. Russo, and H. H. Wolter, Phys. Lett. **B 246**, 337 (1990).

[41] L. Wilets, Y. Yariv, and R. Chestnut, Nucl. Phys. **A 301**, 359 (1978); A. R. Bodmer, C. N. Panos, and A. D. MacKellar, Phys. Rev. **C 22**, 1025 (1980); A. Vicentini, G. Jacucci and V. R. Pandharipande, Phys. Rev. **C 31**, 1783 (1985).

[42] J. Aichelin and H. Stocker, Phys. Lett. **B 176**, 14 (1986).

[43] B. A. Li et al., Phys. Rev. **C 52**, R1746 (1995).

[44] B. A. Li, Phys. Rev. Lett. **88**, 192701 (2002) and refs. Therein.

[45] M. Colonna et al., Phys. Rev. **C 57**, 1410 (1998).

[46] S. Kumar, RK Puri, Phys. Rev. **C 81**, S. Kumar, Rajni, S. Kumar phys. Rev. **C 82**, 024610 (2011).

[47] J. Singh, S. Kumar, and R. K. Puri, Phys. Rev. **C 62**, 044617 (2000); ibid., 65, 024602

(2002).

[48] S. Kumar, Ph.D Thesis 1999, Punjab University, Chandigarh (India).

[49] R. K. Puri, C. Hartnack, and J. Aichelin, Phys. Rev. **C 54**, R28 (1996); P. B. Gossiaux, R. K. Puri, C. Hartnack, and J. Aichelin, Nucl. Phys. **A 619**, 379 (1997).

CHAPTER 2

Methodology

2.1 Introduction

The dynamical transport models employed at intermediate energies are supposed to include the essential collision. The dynamical models can follow the time evolution of nucleons only. These models are termed as “primary models" which generate the phase-space of nucleons. To define the clusters one need “secondary models. This method identifies two nucleons in the same fragment if their centroids are less than some distance. This method is also called as Minimum Spanning Tree (MST) method. Presently the microscopic models can be subdivided into two classes: Those which follow the time evolution of the one-body phase space distribution and those which are based on *n*-body molecular dynamics or cascade schemes. In brief we will discuss the Vlasov-Uehling-Uhlenbeck (VUU) model, Quantum Molecular dynamics (QMD) [6] model and its extension i.e. Isospin Quantum Molecular Dynamic (IQMD) [8] Model in details.

2.2 VUU-Type Model

One of the first microscopic models for the description of relativistic heavy ion collisions Vlasov--Uehling--Uhlenbeck (VUU) model [1] (or BUU [2], LV [3]) which solves the following transport equation for the one-body distribution function f:

$$\frac{\partial f}{\partial t} + v.\nabla_r f - \nabla_r U.\nabla_p f = -\frac{1}{(2\pi)^6}\int d^3p_2\, d^3\dot{p}_2 d\Omega\, \frac{d\sigma}{d\Omega}\, v_{12} \times \{[f f_2 (1-\acute{f}_1)(1-\acute{f}_2) - \acute{f}_1\acute{f}_2 (1-f)(1-f_2)] \times (2\pi)^3 \delta^3 (p + p_2 - p_1' - p_2')\} \quad (1)$$

The l.h.s. of this equation can be derived from the total differential of f with respect to the time by use of the assumptions that the forces can be derived from a potential U. This potential reflects all the real part of the Brückner G-matrix. Usually a Skyrme-parametization of the G-matrix is employed.

$$U = \alpha\left(\frac{\rho}{\rho_0}\right) + \beta\left(\frac{\rho}{\rho_0}\right)^{\gamma} \tag{2}$$

The r.h.s. contains a Boltzmann collision. This part describes the influence of binary hard-core collisions, where the term with ff_2 describes the loss of particles (in a phase space region) and the term with $f_1' f_2'$ the gain term due to collisions feeding the considered phase space region. The delta functions assure the conservation of the four-momentum and the Nordheim-Uehling-Uhlenbeck factors assure the validity of the Pauli principle in the final state of the collision. The cross section $\boldsymbol{\sigma}$ is normally adapted to the free nucleon-nucleon scattering. Here the continuous one-body distribution function f at t=0 is represented by an ensemble of n ($A_P + A_t$), where A_P and A_t denote the number of nucleons of projectile and target, respectively. These particles are propagated under Hamilton's equations of motion with additional stochastic scattering similar to the collisions in cascade models [4]. The Landau-Vlasov model determines f by the overlap of several Gaussians. The collisions are performed in a crossed-event (or full ensemble) method where each particle (independent of its index/event number) may collide with each other particle with a scaled cross section.

The VUU type models succeeded in the description of ``one-body'' observables like collective flow, stopping and particle spectra. However, fluctuations and correlations, such as the formation of fragments or the description of two-particle correlations in relativistic heavy ion collisions, are beyond the scope of a transport model based on a one-body distribution function [5]. This was one of the motivations for the development of the Quantum Molecular Dynamics model (QMD) [6].

2.3 Quantum Molecular Dynamics (QMD) Model

The QMD [6] model is a n body theory which simulates heavy ion reactions at intermediate energies on a event by event basis. The collisions are performed in a point-particle sense in a similar way as in VUU or cascade: Two particles collide if their minimum distance d, i.e. the minimum relative distance of the centroids of the Gaussians during their motion, in their CM frame fulfils the requirement:

$$d \leq d_0 = \sqrt{\frac{\sigma_{tot}}{\Pi}}, \qquad \sigma_{tot} = \sigma\left(\sqrt{s}, \text{type}\right). \tag{3}$$

where the cross section is assumed to be the free cross section of the regarded collision type (N-N, N-Δ, ...). In the original QMD version only nucleons and Deltas are regarded without explicit treatment of the isospin. Later versions (which will be discussed later) include nucleons, deltas, N*and pions with their isospin components. For unknown cross sections isospin symmetry and time reversibility is assumed. Particular versions use also the one boson exchange model (OBE). If the particles scatter, the direction of the final momenta will be distributed randomly according to the given polar angle distribution in the two particle CM-system. For elastic scattering the distribution is taken from [7]

$$\frac{d\sigma_{el}}{d\Omega} \sim \exp\left(A(s)t\right). \tag{4}$$

Where t is $-q^2$, the squared momentum transfer and $\sqrt{s}$ is the c.m. energy in GeV.

A reduction of the effective cross section is obtained by the ``Pauli-blocking''. For each collision the phase space densities in the final states are checked in order to assure that the final distribution in phase space is in agreement with the Pauli principle. Since the phase space in QMD is not discredited into elementary cells and for getting smoother distribution functions the following procedure is performed. The insufficiencies of the Pauli blocking algorithm in the standard QMD become important at energies below 25 MeV/nucleon.

2.4 Isospin Quantum Molecular Dynamics (IQMD) Model

Isospin helps to extract the information of the EOS of neutron rich matter, especially the density dependence of the nuclear symmetry energy. Isospin is a

factor which differentiates between the neutron and proton inside the nucleus on the basis of the charges and makes possible interactions between the n-n, p-p and n-p. Isospin degree of freedom enters in term of isospin-dependent physical quantities such as the isovector (symmetry) potential, and isospin-dependent in-medium nucleon-nucleon (NN) cross-sections and Pauli blocking. The dynamics in HIC at intermediate energies can be described by the three important components namely

1) The mean field.

2) Two-body collisions.

3) Pauli blocking.

So it is essential that these three components should reasonably include the 'isospin degree of freedom'. The QMD [6] model is a classical aspect which is a true N-body theory, is capable of treating both the compression and fragments formation, because the time evolution of the system is determined by the classical canonical equation of motion. However QMD [6] model include many important quantum features like Pauli blocking, stochastic collisions, sub-threshold particle production, etc. In IQMD [8], it is also important that, in initialization of target and projectile nuclei, the samples of neutrons and protons in the phase space should be treated separately since there exist a large difference in density distribution of neutrons and protons for the nuclei far from the β stability line. The IQMD model has been used successfully for the analysis of the observables from low to relativistic energies [8]. The Isospin degree of freedom enters the calculations via both cross sections and mean field.

From this enumeration one may assume that there are three major parts in the numerical realization which may play an important role for the solution of the transport equation, namely the initialization, the propagation and the collision. For the propagation the description of the potential (or to be more exact of the real part of the Brückner G-matrix) is of crucial importance. Which we discuss in detail as

2.4.1 Initialization

It is very important to make sure that our initialization does not affect the stability of cold nuclei. In the IQMD model, the neutrons and protons are distinguished from each other in the initialization of projectile and target nuclei. The neutron and proton density for the initial projectile and target nuclei are determined by Skyrme-Hartree-Fock method. The IQMD model treats different charge states of nucleons, deltas, and pions explicitly. In this model the baryons are represented by Gaussian –shaped density distributions

$$f_i(\vec{r},\vec{p},t) = \frac{1}{\pi^2\hbar^2} e^{-[\vec{r}-\vec{r}_i(t)]^2\frac{1}{2L}} e^{-[\vec{p}-\vec{p}_i(t)]^2\frac{2L}{\hbar^2}} \quad (5)$$

Where $r_i(t)$, $p_i(t)$ define the classical orbit or the centre of the Gaussian wave packet in the phase space. The centroid of the Gaussians in a nucleus are randomly distributed in a phase space sphere ($r \leq R \; and \; p \leq p_F$) with $R = 1.12A^{1/3}$fm corresponding to a ground state density of ρ_o= 0.17fm^{-3}. The Fermi momentum p_F depends upon the ground state density. For ρ_o= 0.17fm^{-3}, the value of $p_F \approx$ 268 MeV/c. The momenta are uniformly distributed within a momentum sphere without any local constraints. Therefore the nucleons near the surface, because of low potential energy, are unbound initially. This possibility however gives a reduced binding energy per nucleon as compared to Weizsacker mass formula. So the initialized nuclei are less stable against spurious particle evaporation compared to oriented QMD model. Recently studies have been done to see the effect of width of the Gaussian wave packet on fragmentation using QMD model [6]. It was observed that the variation of the width (L) has a sizable effect on the clusterization. A broader Gaussian binds more nucleons into a fragment. As a result the fragment turns much heavier. The interaction range parameter *L* influences the interaction density for finite systems. For (homogeneous) infinite nuclear matter the density (and thus the potential energy) does not depend any more on the extension of the Gaussian wave packets. Thus, the equation of state of infinite nuclear matter is independent of *L*. Thus even two parameterizations which yield the same EOS may produce different results for the reaction of two heavy ions. Therefore we have to adjust *L* to have reasonable surface properties. In order to allow a physical interpretation *L* should be in the order of the size one expects for the range of the nuclear interaction. There exists a range of values for *L*, which allows fixing these

properties. Larger values of *L* increase the effective range of the interaction and thus lead to some smearing of fluctuations, which are stronger for more located wave packets (small values of *L*). The Gaussian width can be regarded as a description of the interaction range of a particle. Its influence disappears for infinite nuclear matter whereas for finite systems it may play a non negligible role. In IQMD the Gaussian width can be used as an optional input parameter. The system dependence of *L* in IQMD has been introduced in order to obtain maximum stability of the nucleonic density profiles. As an example for Au + Au a value of L = 8.66 fm^2 is chosen, for Ca + Ca and lighter nuclei L = 4.33 fm^2.

2.4.2 Propagation

These nucleons propagate under the influence of mean field. This process is termed as propagation. The successfully initialized nuclei are then boosted towards each other with the proper centre of mass velocity using relativistic kinematics. The centre of each distribution moves along the Coulomb trajectories. The nucleons of target and projectile interact via two and three body Skyrme forces and the Yukawa potential. The isospin degree of freedom is treated explicitly by employing a symmetry potential and explicit Coulomb forces between the protons of colliding target and projectile. All this provide us a correct distribution of protons and neutrons within the nucleus.

The Hamilton equations of motion for the propagation of hadrons are

$$\frac{dr_i}{dt} = \frac{d\langle H\rangle}{d\,p_i} \tag{6}$$

$$\frac{dp_i}{dt} = -\frac{d\langle H\rangle}{d\,r_i} \tag{7}$$

2.4.3 Collision

Whenever a collision occurred, in the phase space we assume that each nucleon occupies a six dimensional sphere with a volume of h^3/2 and then calculate the phase volume V, of the scattered nucleons being occupied by the rest nucleons with the same isospin as that of the scattered ones. Then we compare 2V/h^3

with a random number and decide whether the collision is blocked or not. So the Pauli blocking is isospin dependent. Pauli blocking of neutron and proton is treated separately. In IQMD model, two different parameterizations of N-*N* cross sections may be used optionally. One of the parameterization of Cugnon (σ_{Cug}) cross section, which is the isospin independent, and the other is the experimental parameterization σ_{exp} which is isospin dependent. It is shown that for experimental parameterization at energies lower than 300 MeV/nucleon, the neutron-proton cross section is about three times larger than the neutron-neutron or proton-proton cross section.

2.4.4 Potential used in IQMD

A total Hamiltonian function with a kinetic energy T and a potential energy V is given by

$$\langle H\rangle = \sum_i \frac{{p_i}^2}{2m_i} + \sum_i \sum_{j>i} \int f_i(\vec{r},\vec{p},t) V^{ij}\left(\overrightarrow{r'},\vec{r}\right) \times f_j(\overrightarrow{r'},\overrightarrow{p'},t) d\vec{r} d\vec{r}' d\vec{p} d\vec{p}' \qquad (8)$$

The potential in equation is the sum of the following specific elementary potentials,

$$V = V_{Sky} + V_{Yuk} + V_{Coul} + V_{mdi} + V_{loc} \qquad (9)$$

With a local hard core repulsion,

$$V_{loc} = \sum_i \sum_{j>i} t_1 \delta(\vec{r}_i - \vec{r}_j) + \sum_i \sum_{j>i} \sum_{k>j} t_2 \delta\left(\vec{r}_i - \vec{r}_j\right) \delta(\vec{r}_i - \vec{r}_k) \qquad (10)$$

The Yukawa short-range term,

$$V_{Yuk} = \sum_i \sum_{j>i} t_3 \frac{\exp\left(|\vec{r}_i - \vec{r}_j|/\mu\right)}{\left(|\vec{r}_i - \vec{r}_j|/\mu\right)} \qquad (11)$$

The Yukawa potential V_{Yuk} in IQMD is very short ranged and weak ($\mu = 0.4$ fm). Additional attractive Yukawa forces hence modify the EOS. Yukawa forces stabilize the nuclei because of the increase of the interaction range as compared to a δ-like Skyrme potential. Thus nucleons notice earlier that they will arrive at the surface and are more effectively deaccelerated without this potential. In addition the

fluctuations are reduced. The Coulomb term with only a mean value for the nucleon charge because in QMD the isospin of the particles is not included,

$$V_{Coul}=\sum_i \sum_{j>i} \frac{Z_i Z_j e^2}{|\vec{r}'-\vec{r}|} \quad (12)$$

And the momentum dependent interaction

$$V_{mdi} =\sum_i \sum_{j>i} t_4 \ln(1+t_5(\vec{p}_i - \vec{p}_j)^2)\delta(\vec{r}_i - \vec{r}_j) \quad (13)$$

The IQMD-model offers rather stable density distributions and good energy conservation, however at the price of nucleon evaporation and improper binding energies (E_{bind} ≈ 4-5 MeV/nucleon for heavy nuclei instead of 8 MeV/nucleon). In addition to the potential used in QMD, a symmetry potential between protons and neutrons corresponding to the Bethe-Weizsacker mass formula has been included

$$V_{Sym}^{ij}= t_6 \frac{1}{\rho_o} T_3^i T_3^j \delta\left(\vec{r}_i^{\,\prime} - \vec{r}_j\right) \quad (14)$$

Where T_3^i and T_3^j denote the isospin projections of particles *i* and *j*. Other baryonic potentials like V_{Sym}^{ij} and V_{mdi} are defined isospin-independent like in all other flavors. The parameters are propagated under the total interaction calculated by the Hamiltonian equations of motion (5) and (6). Parameters used in equation (10) to (13) are shown in table below:

IQMD parameters	Values use
t_3	15 MeV
t_4	1.57 MeV
t_5	5.10^{-4} MeV^{-2}
t_6	25 MeV
μ	0.4 fm

Table 2.1: IQMD parameters used in equation (10) to (11)

To understand little bit more about IQMD model, let's take a glance on IQMD code

The main parameters which are included in IQMD model are radius, cross section, time step, multiplier to delta decay width, switches, equation of state, random number, initialisation Gaussian width and symmetry energy. Some of them having certain particular value some parameters values are change according to need.

In IQMD model isospin effect is taken into consideration, so in IQMD model mass number and atomic number of projectile and target are very important, here each proton and neutron of projectile and target collide with each other. The number of parallel event is '1' i.e. only one n/p interaction between target and projectile take place at one time. There are lot of switches we note only those in which first collision to be allowed for a nucleon will be a collision with a nucleon that is either of the other nucleon or has already collided. Time step is number of time step that are calculated for each run we take the size of time step in fm/c the reaction time will thus be the number of time step × time step width, then we have printout step. It tells us after how many step the output will be yield for e.g. if we take 90 as printout step then output will be yield after 90,180,270 ... step.

In IQMD model frame of reference play a vital role. In general there are four frames of reference

1. NN
2. Center of mass frame (CM)
3. Laboratory frame of reference (LAB)
4. Projectile frame (PRO)

A frame of reference in physics may refer to a coordinate system or set of axes within which to measure the position, orientation, and other properties of objects in it, or it may refer to an observational reference frame tied to the state of motion of an observer. It may also refer to both an observational reference frame and an attached coordinate system, as a unit. Center of momentum frame is the center of mass frame. It is an inertial frame in which the center of mass (which is a physical point) is at the origin at all times. In all CM frames, the center of mass is at rest, but it may not

necessarily be at rest at the origin of the coordinate system. The laboratory frame of reference, or lab frame for short, is a frame of reference centred on the laboratory in frame of reference. PRO is known as projectile frame. In NN the projectile and target have same momentum/nucleon due to high energy and particles production due to this reason we generally used NN frame to study the fragment.

Radius parameter, it is by default in IQMD model taken 1.12 as per Rutherford scattering. This is the radius parameter of the initialisation of projectile and target. Their radii will be calculated according to

$$R = R_0 A^{0.33}$$

2.5 Method of clusterization

2.5.1 Minimum spanning tree (MST) method

One of the most extensively used methods to clusterize the nucleons is MST [9] (Minimum spanning tree). According to this method two nucleons share the same fragment if their centroids are closer than a distance d_{min},

$$\left|\vec{r}_i - \vec{r}_j\right| \leq d_{min}$$

Where $\vec{r}_i$ and $\vec{r}_j$ are the spatial positions of both nucleons. The value of d_{min} can vary between 2-4 fm. It has small effect on multifragmentation. However, this method can not address the question of time scale as it will give a big fragment at the time of highest density when the interactions between the nucleons are still active. This method can only be used to analyze asymptotic configuration in which the fragmenting system can be viewed as a very dilute mixture of free particles and almost equilibrated fragments.

2.6 REFERENCES

[1] H. Kruse, B. V. Jacak, and H. Stöcker. Phys. Rev. Lett. **54**, 289 (1985).

[2] G.F. Bertsch, H. Kruse and S. Das Gupta. Phys. Rev. **C 29**, R673 (1984).

[3] C. Gregoire, B. Remaud, F. Sebille, L. Vinet, and Y. Raffray, Nucl. Phys. **A 465**, 317 (1987).

[4] Y. Yariv and Z. Frankel. Phys. Rev. **C 20**, 2227 (1979).

[5] P.B. Gossiaux, D. Keane, S. Wang, and J. Aichelin, Phys. Rev. **C 51**, 3357 (1995).

[6] R K Puri, C Hartnack and J. Aichelin, Phys. Rev. **C 54**, R 28 (1996); P.B. Gossiaux et al, Nucl. Phys. **A 619**, 379 (1997); R K Puri and J. Aichelin, J. Comp. Phys. **162**, 245 (2000); Y K Vermani, S Goyal and R K Puri, J. Phys. G: Nucl. Part. **36**, 105103 (2009); Y K Vermani and R K Puri, Eur. Phys. Lett. **85**, 62001 (2009).

[7] J. Cugnon, T. Mizutani and J. Vandermeulen. Nucl. Phys. **A 352**, 505 (1981).

[8] C Hartnack et al, Eur. Phys. J. **A 1**, 151 (1998); D T Khoa et al, Nucl. Phys. **A 548**, 102 (1992); E Lehmann, R K Puri, A Faessler, G Batko and S W Huang, Phys. Rev. **C 51**, 2113 (1995); R K Puri et al, Nucl. Phys. **A 575**, 733 (1994); C Fuchs et al, J. Phys. G: Nucl. Phys. **30**, 219(1993) ; E Lehmann et al, Prog. Part. Nucl. Phys. **30**, 219 (1993); E Lehmann et al, Z. Phys. **A355**, 55 (1996).

[9] J Singh, S Kumar and R K Puri, Phys. Rev. **C 62**, 044617 (2000); S Kumar and R K Puri, ibid. **58**, 1618 (1998); Y K Vermani, S Goyal and R K Puri, ibid. **79**, 064613 (2009).

CHAPTER 3

EFFECT OF SYMMETRY ENERGY ON FRAGMENTS

3.1 Introduction

Symmetry energy plays role in fragmentation. In Those situations if matter is highly compressed, the nucleon-nucleon correlations are already broken due to violent nucleon-nucleon collision. A very few attempts exists in literature which deals with systematic study of the mass dependence of the multifragmentation with density dependent symmetry energy. The evolution of lepton profiles, cooling process and the neutrino fluxes in neutron stars depend strongly on the nuclear symmetry energy [1, 2]. Therefore, more and more attention has been paid to study the symmetry energy in both infinite nuclear matter and finite nuclei.

We have simulated 1000 events involving the symmetric reactions of $_{10}Ne^{20}+_{10}Ne^{20}$, $_{20}Ca^{40}+_{20}Ca^{40}$, $_{40}Zr^{91}+_{40}Zr^{91}$, $_{54}Xe^{131}+_{54}Xe^{131}$ and $_{79}Au^{197}+_{79}Au^{197}$ for incident energies 50, 100, 200, 400, 600, 1000 MeV/nucleon using different collision geometries with different density form of dependent symmetry energy. For the analysis, soft as well as soft momentum dependent (SMD) equation of state with compressibility K = 200 MeV is used [3]. By using the symmetric (colliding) nuclei, system size effects can be analyzed without varying the asymmetry mass of the system. It is worth mentioning that the experimental studies by the MSU mini ball and ALADIN groups varied the asymmetry of the reaction whereas FOPI experiments [4] are performed for the symmetric colliding nuclei only.

In the section 3.2, we first discuss the phase space of Au +Au nucleons followed by the time evolution at energy 50 MeV/nucleon. Then in 3.3 section we analysis the effect of symmetry energy with normal density by time evolution at energy 50 and 400 MeV/nucleon. In section 3.4 the time evolution of allow collision is compare at energy 50 and 400 MeV/nucleon. While in section 3.5 we analysis multiplicity at different time-step at above two energies. 3.6 show the effect of energy

on the multiplicity of the different colliding nuclei. In section 3.8 we point the effect of cross-section on symmetry energy.

3.2 Phase space

A plot of position and momentum co-ordinates as a function of time is called a phase plot or a phase diagram. A space in which all possible states of a system are represented, with each possible state of the system corresponding to one unique point in the phase space. For mechanical systems, the phase space usually consists of all possible values of position and momentum variables. In a space every degree of freedom or parameter of the system is represented as an axis of a multidimensional space.

In the Fig 3.2 thousands of event were simulated for the neutron-rich reaction of $^{197}Au_{79}$ +$^{197}Au_{79}$ at incident energy 50 MeV/nucleon using soft and hard equation of state along with isospin dependent free and constant nucleon-nucleon cross-sections. The geometry of the collision is varied between the most-central to peripheral one. We note that irrespective of the symmetry energy, central collisions lead to complete spherical distribution of particles, indicating, spreading of the nucleons in all directions. In contrast, the momentum space is less affected. On the basis of mass number the fragments are classified as

1. Free nucleons [1≤A≤1]
2. Light mass fragments (LMF's) [2≤A≤4]
3. Medium mass fragments(MMF's) [5≤A≤9]
4. Intermediate mass fragments(IMF's)[5≤A≤A_{tot}/(3 or 6)]

Since free nucleons as well as LMF's originate from the mid-rapidity region, they are better suited for studying the degree of stopping reached in a heavy-ion collision. On the other hand, IMF's seems to originate either from the target or from the projectile region, therefore, are the remnant/residue of the spectator matter.

The part of target and projectile which are participating in the collision are called as participants and rest are called as spectator. As shown in Fig. 3.1 fire ball is known as participant and spectators are shown by semicircles. In central collisions, the

dominance of the participant nucleons, where as peripheral collisions are dominated by the spectator matter.

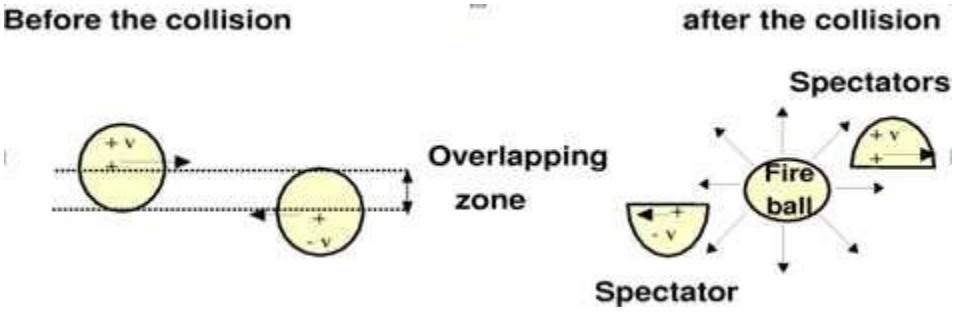

Fig 3.1: Schematic diagram of the spectator and participant part of colliding nucleons.

Fig.3.2 and 3.3 represents the phase space of position and momentum co-ordinate respectively. For a single event of $_{79}Au^{197}$ + $_{79}Au^{197}$ collision at different time-steps for both hard and soft equation of state is analysed. Using different parameter sets corresponding to different compressibility values ranging from about 200 MeV (less repulsive), a so-called soft EOS up to about 380 MeV (more repulsive), so called hard E*OS*. As we know the features of EOS in intermediate energy heavy-ion collisions can be inferred from multifragmentation, collective flow and nuclear sttoping. On the other hand, NEOS at higher incident energies is characterized by the production of sub-threshold particles [5] and their isospin dependence [6]. From fig. 3.2 there is no large effect on colliding nuclei till time-step 30 fm/c, after that large expansion or we can say nucleon scattering is observed more in hard EOS as compare to soft EOS. The different in both EOS is increase with increase in incident energy [3, 7]. The difference in compressibility factor for both EOS in position phase space is more dominate then the momentum phase space as shown in Fig. 3.3.

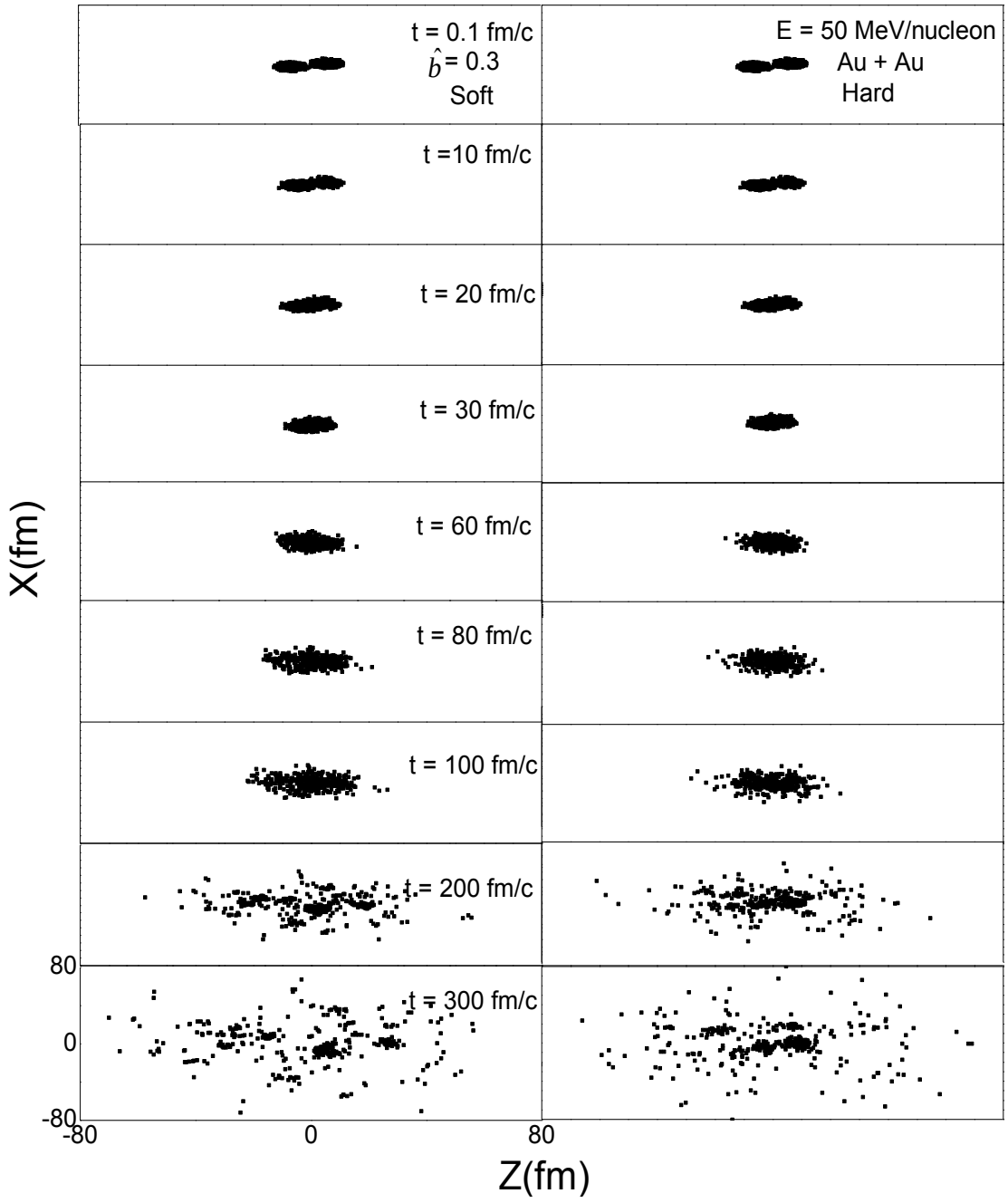

Fig. 3.2: The time evolution of phase space of Au+Au reaction at scaled impact paramrte 0.3 and incident energy is 50 MeV/nucleon. This plot is projection of X-Z plane. Left panel shows the phase with soft EOS and right panel shows the with hard EOS.

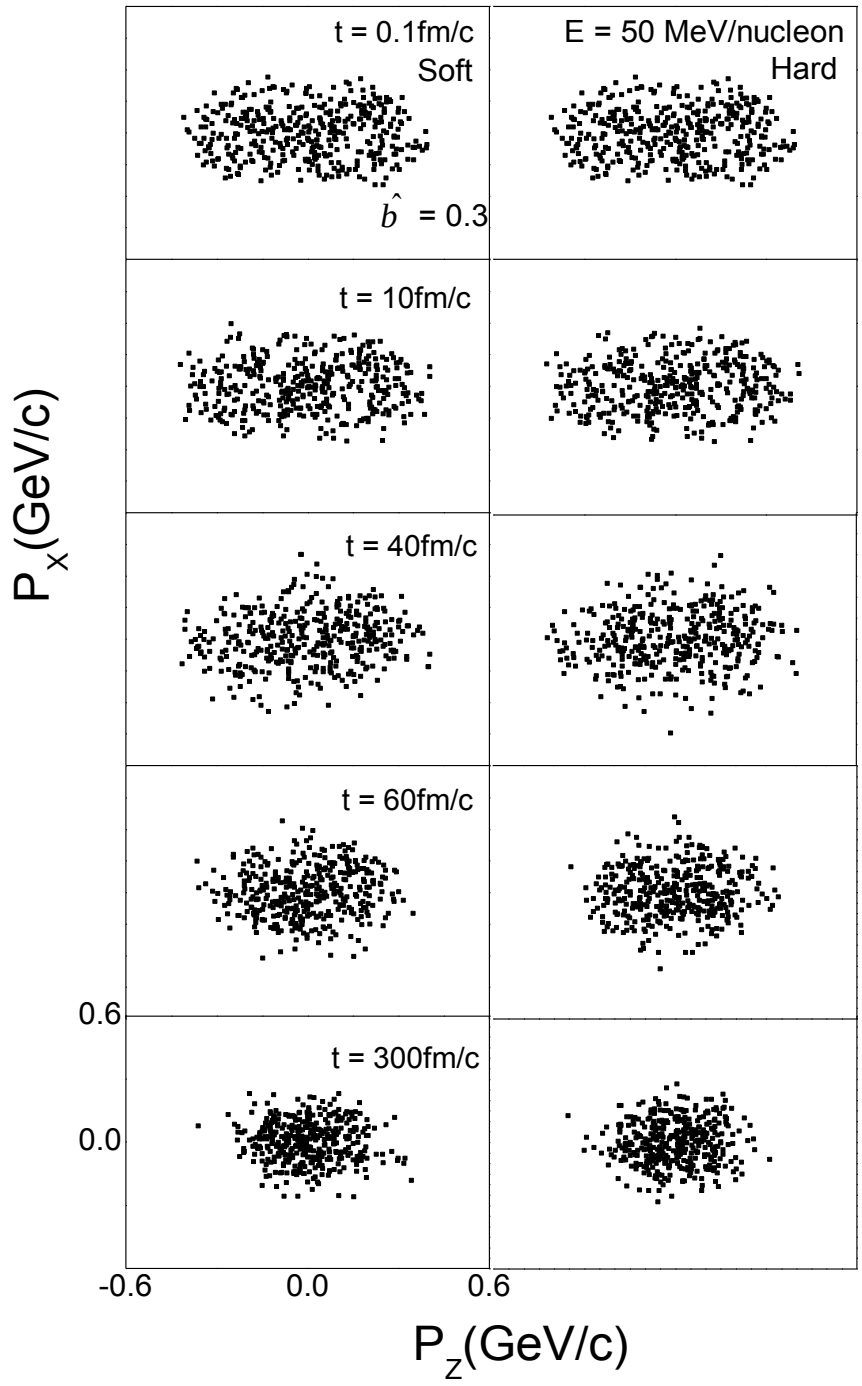

Fig. 3.3: The time evolution of momentum space of Au+Au reaction at scaled impact parameter 0.3 and incident energy is 50 MeV/nucleon. Left panel shows the momentum space with soft EOS and right panel shows the momentum space with hard EOS.

3.3 Time evolution of density

The density of the environment surrounding the nucleons of a fragment plays crucial role in deciding the physical process behind their formation. In

Fig.3.4 and Fig.3.5, we display the average density $< \rho/\rho_0 >$ reached in a typical reaction as a function of the time. The average nucleonic density $< \rho/\rho_0 >$ is calculated as (1)

$$< \rho/\rho_0 > = \langle \frac{1}{A_T + A_P} \sum_{i=1}^{A_T + A_P} \sum_{j=1}^{A_T + A_P} \frac{1}{(2\pi L)^{3/2}} \cdot exp[-(\vec{r_i} - \vec{r_j})^2/2L] \rangle, \quad (1)$$

With r_i and r_j being the position coordinates of i^{th} and j^{th} nucleons, respectively. We here display the average density at incident energies of 50 and 400 MeV/nucleon at time-step 0.1, 10, 20, 40, 60, 80, 100, 200, 300 fm/c for central collisions using soft EOS. One finds that the saturation density in central collision is nearly independent of the form of EOS. The central as well as peripheral collisions (at low incident energy) preserve most of the initial correlations and hence a small change in the density profile occurs. This trend turns to a sharp decrease at higher incident energies as shown in Fig.3.5. This is due to the fact that higher incident energies destroy most of the initial correlations among nucleons, leading to highly unstable compressed zone, which does not sustain for a longer time and as a result fast emission of nucleons occur. It is also observed experimentally that a little change in fragmentation yield takes place beyond 400 MeV/nucleon [8].

From two Figures we see that the time evolution of density remain same for different symmetry energy values rather than value dependent upon incident energy. We see the different line for different systems. From the figs. it is also observed that heavier colliding nuclei are more compressed as compared to lighter one. This compression stage also sustains for a longer time in heavier nuclei as compared to lighter one. We observed that below 60 fm/c large due to collision. We see there is gradual decrease in density due to expansion of the nuclear matter. Naturally, the saturation time of the density depends strongly on the masses of the colliding nuclei. The saturation density in case of heaviest colliding nuclei is less compared to lighter colliding nuclei, because after compression nuclear matter expands abruptly in the case of heavy nuclei. The symmetry energy E_{sym} (ρ, T) represents a very good accuracy the energy cost per nucleon to convert all the protons to neutrons in symmetric nuclear matter at the density ρ and temperature T. Study of its density and energy dependence is of almost contemporary importance.

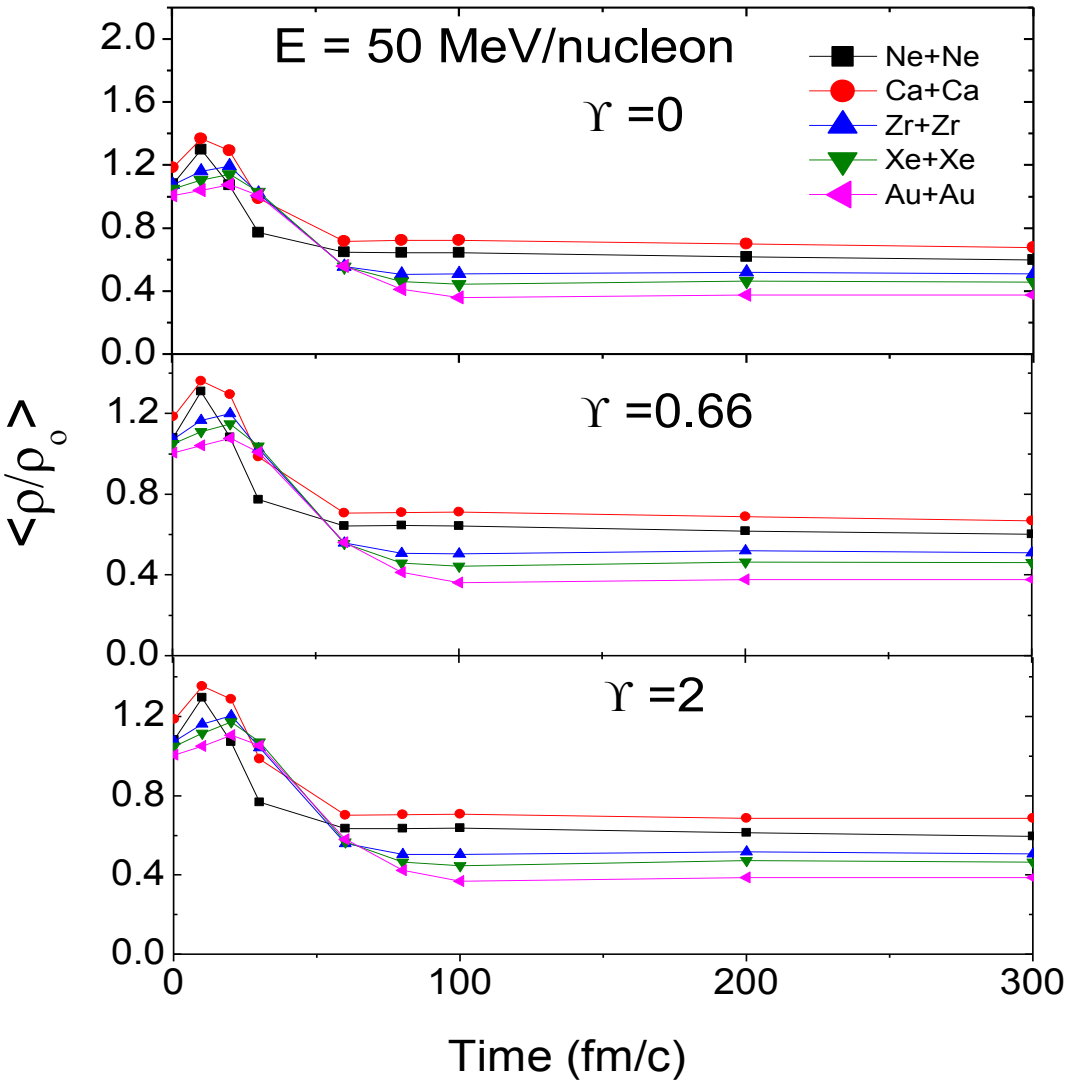

Fig. 3.4: Average density <ρ/ρ$_O$> as a function of the time for different colliding nuclei at energy 50 MeV/nucleon at different ϒ values for scaled impact parameter 0.3.

3.4 Time evolution of allowed collision

The time evolution of the allowed collisions is displayed under the same conditions as density profile. The collision profile is in one to one ratio with the density profile. As there is no effect of ϒ value in density profile similarly there is no effect of ϒ value in allows collision profile. Generally, collision rate depends on the participant zone and incident energy.

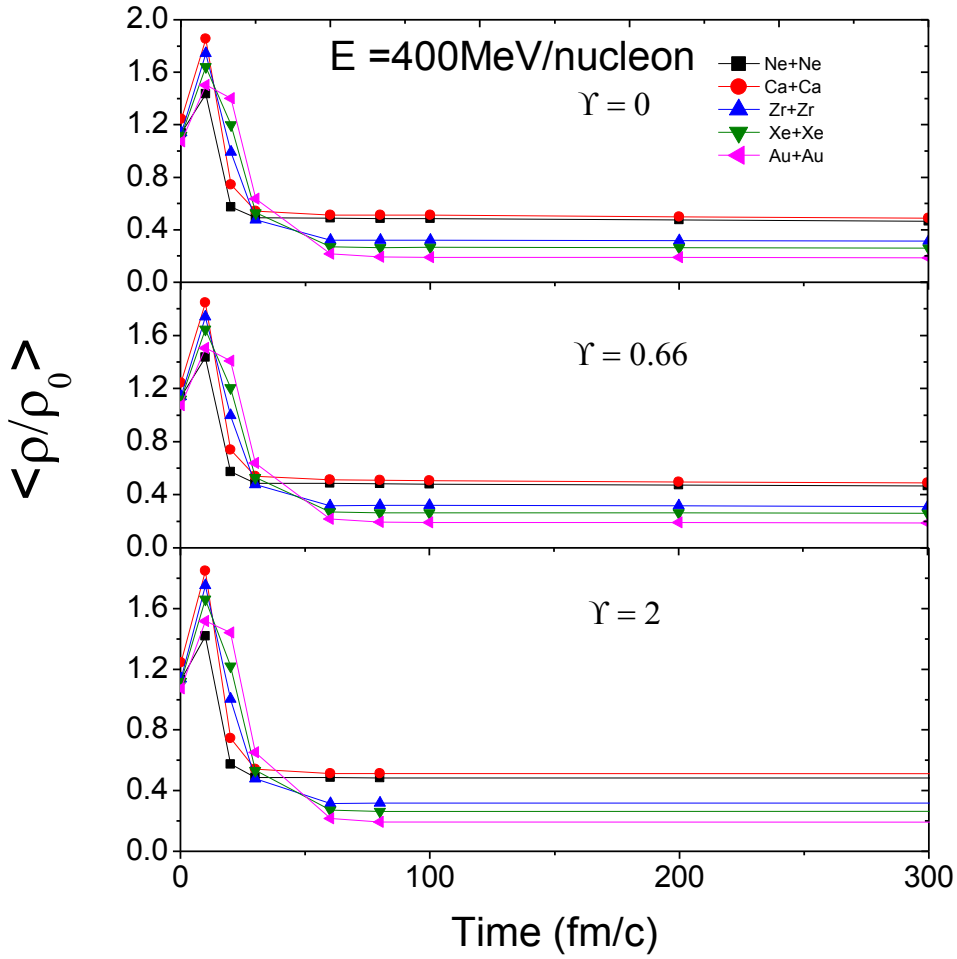

Figure 3.5: Average density <ρ/ρ$_0$> as a function of the time at energy 400 MeV/nucleon at different ϒ values for b = 0.3 for different colliding nuclei.

From Fig.3.6, we observe allowed collision increase with increase in incident energy from 50 and 400 MeV/nucleon. Rate of collision at low energy vary less as compare to the rate of collision at high energy because Pauli blocking dominate at low energy. Collision rate is found to increase almost 10 times with the probability of breakup of initial correlations among the nucleons. This is due to less influence of Pauli blocking at high energy. To see the mass effect from figure, we observed that the maximum collision rate for central Au+Au system at 400 MeV/nucleon is about 46, whereas it is 4.5 at 50 MeV/nucleon. The maximum collision for lightest participant i.e. Ne+Ne system at 400 MeV/nucleon is about 4.5 and at 50 MeV/nucleon is 1.

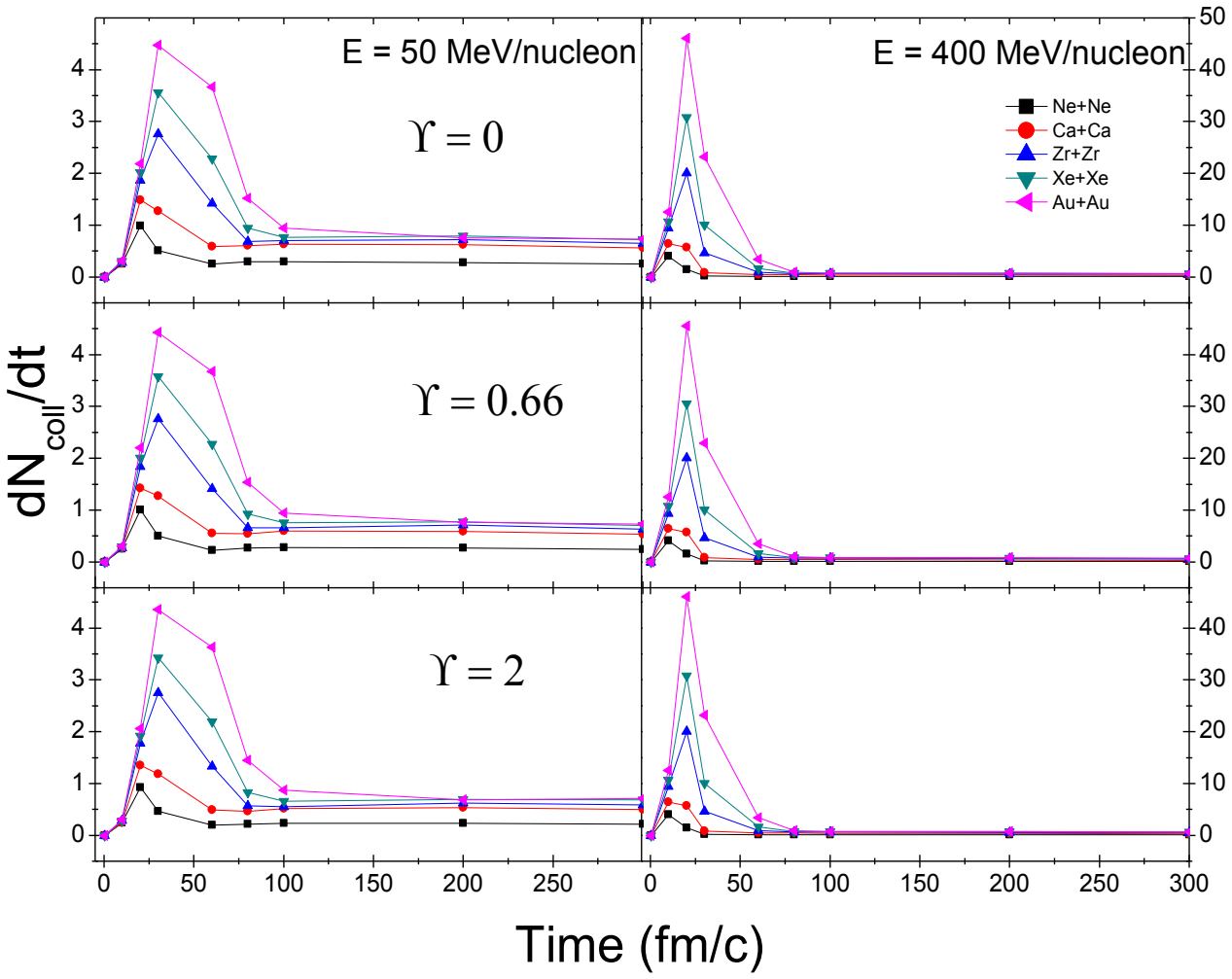

Fig. 3.6: Time evolution of collision rate dN_{coll}/dt at incident energy 50 and 400 MeV/nucleon in left and right panel respectively at different ϒ values.

This change in collision rate can be explained by compressibility as in density profile. Number of collision increases with increase in neutron and proton in the colliding nuclei.

3.5 Time evolution of multiplicity

As we know, measurements of fragments are always done at the saturation time in a reaction. In Fig. 3.7 we display the time evolution of fragmentation. The reaction time is t = 0.1, 10, 20, 40, 60, 80, 100, 200, 300 fm/c. It will be of interest to see the final state fragment distribution has size dependence. The time evolution of free nucleons (FN) [1 ≤ A ≤ 1], light mass fragments (LMF's)[2 ≤ A ≤ 4], medium mass

fragments (MMF's) [5 ≤ A ≤ 9] and intermediate mass fragments (IMF's) [5 ≤ A ≤ A_{tot}/x, where x = 3 for lighter nuclei (Ne, Ca) and x = 6 for heavy nuclei (Zr, Xe, Au) is displayed for central collision is zero at two incident energies 50 and 400 MeV/nucleon. In this figure we take 200 fm/c as freeze out time. The freeze out is that time beyond this time fragments do not decay further. In some cases, the multiplicity of fragments continues to change even at 200 fm/c. We in fact do not know whether the contribution after 200 fm/c is a real one or just spurious yield due to the de-stabilization of fragments. Therefore, we stop the reaction at 200 fm/c.

On see the effect of incident energy and mass number on number of free nucleon and light mass fragments generated, it increases with increase in incident energy as shown in section 3.6. As number of FN at energy 50 MeV/nucleon for Au + Au is about 90 and at 400 MeV/nucleon is about 220. We see number of FN increase continuously for heavy nuclei and there is no saturation while for light nuclei there is saturation after 200 fm/c. The LMF almost one-forth in number as compare to FN. In LMF freeze out time at energy 50 MeV/nucleon is at 200 fm/c, but at higher energy it shifts towards the 100 fm/c. The multiplicity of MMF's and IMF's at 400 MeV/nucleon shows a decrease due to decay of excited fragment at 400 MeV/nucleon.

A lot of efforts are available in the literature to pin down the importance of system size effects without momentum dependent interactions. This includes the temperature as well as density, flow of nucleons/fragments, disappearance of nuclear flow, particle production and multifragmentation etc. The study of the mass dependence in the evolution of the density and temperature reveals that maximum temperature is insensitive towards the mass of the system. However, the maximum density scales with the size of the interacting system [9]. The hot and dense matter formed in heavy ion collision lasts longer in heavier colliding nuclei compared to lighter colliding nuclei [9]. Interestingly, equation of state also depends on the size of the system. From the Figure, we analyse that all the fragments shows same curve till 60 fm/c, there is no mass effect till 60 fm/c. MMF is almost 5 times less than LMF's. Effect of multiplicity for Ca + Ca on time-step 50, 100, 200, 300 fm/c is studied in the ref [10]. If we see the incident energy effect on the number of MMF we find that at 50 MeV/nucleon the slope of MMF's is positive and we get freeze out time at 200 fm/c

while MMF at energy 400 MeV/nucleon we get a positive slope till a particular point depending upon mass then we get negative slope as shown in Fig. 3.7.

In case of IMF we find that there is drastic change in the behaviour of at low energy as compare to high energy. At 100 fm/c time-step the number of IMF is very less then number of IMF increase at 200 fm/c because they originate from the decay of largest fragment. The IMF will give us possibility of looking for fusion in colliding nuclei, whereas the emission of free nucleons will show the disassembly of the matter.

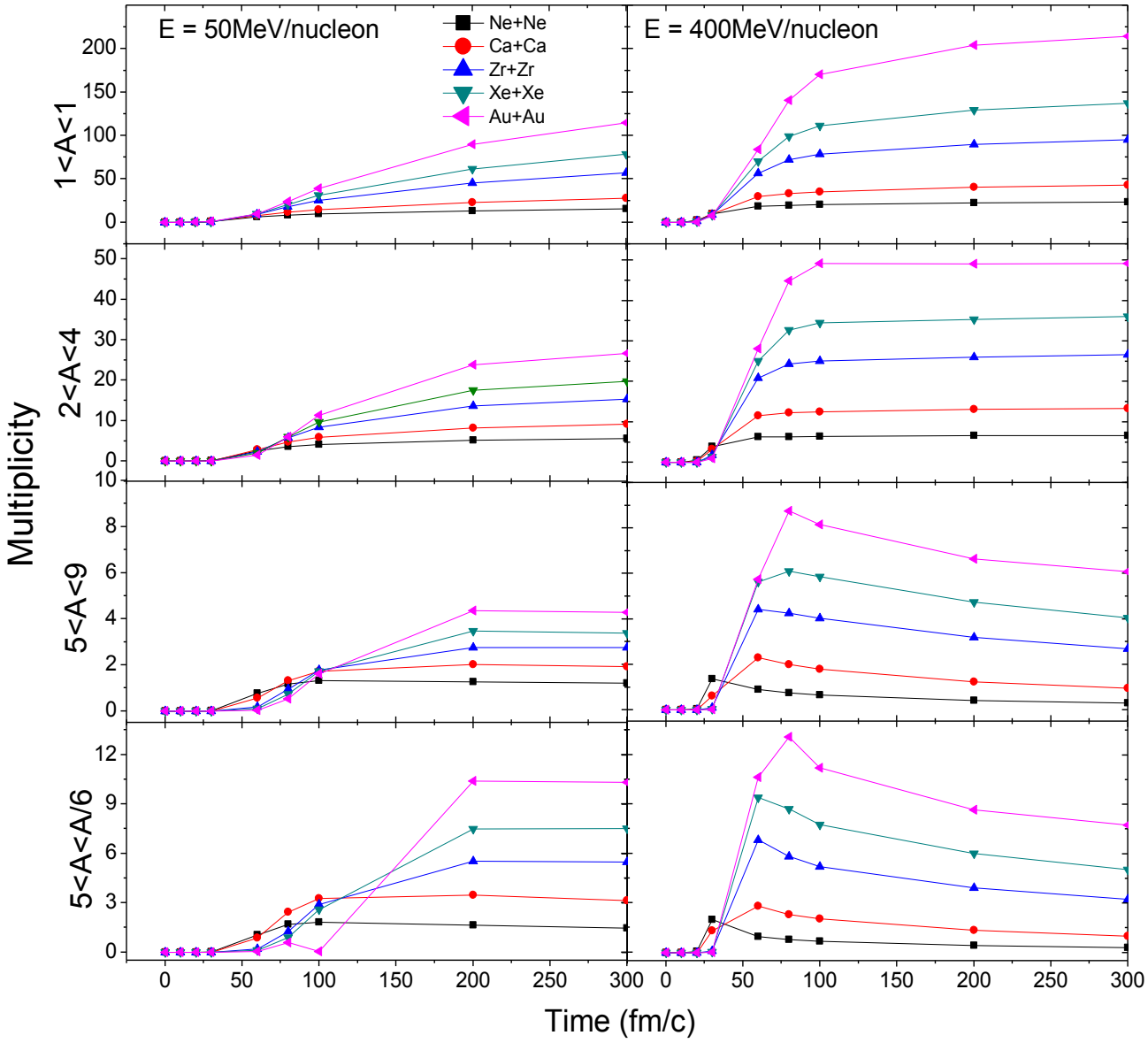

Fig. 3.7: Time evolution of multiplicity of FN's, LMF's, MMF's and IMF's at energy 50 MeV/nucleon in left panels and 400 MeV/nucleon in right panels for γ = 0.

3.6 Effect of incident energy on multiplicity of different nuclei

In above Fig. 3.7 we observe the time evolution on multiplicity and see the effect of incident energy only at 50 and 400 MeV/nucleon. In Fig. 3.8-3.10 we see the effect of incident on FN, LMF, IMF at different symmetry energies. The effect of ϒ is about 10% on fragment formation [11]. But incident energy plays an important role in the formation of fragments. The universal behaviour of increase in multiplicity of fragments with the size of the system is observed in the presence of static as well as momentum dependent interactions.

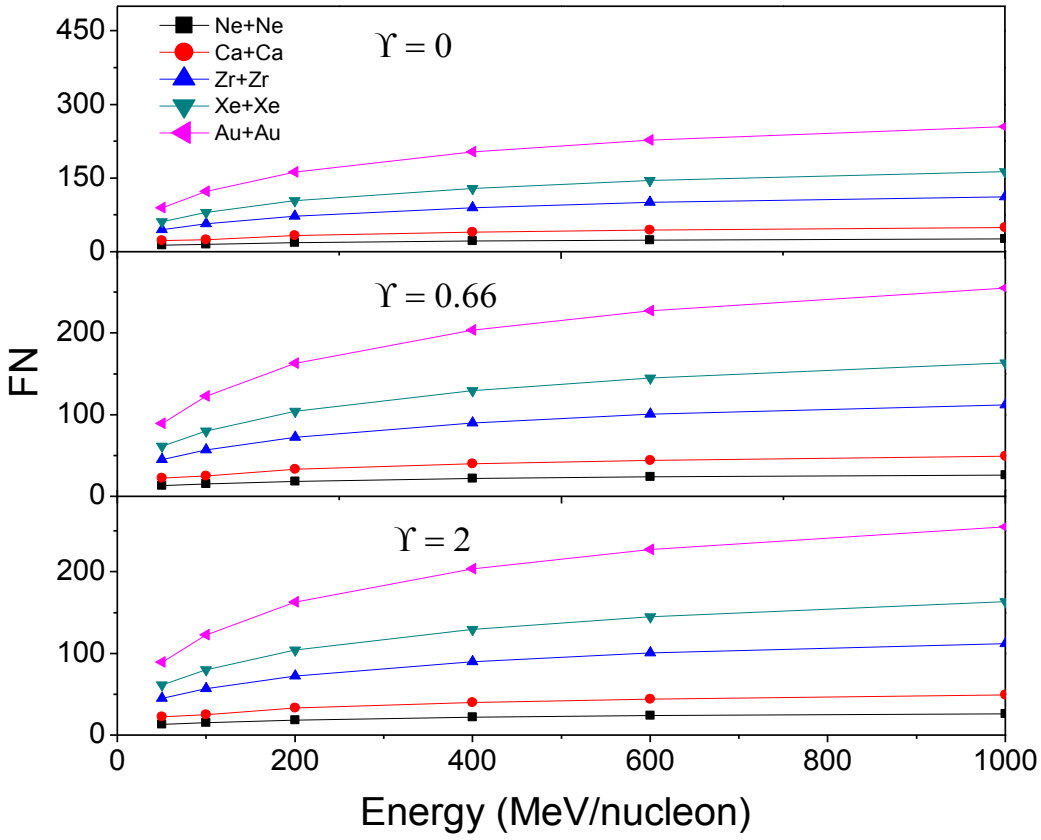

Fig. 3.8: Effect of incident energy on free nucleon of different colliding nuclei for central collision.

The most prominent feature of the multifragment decay is the universality of the fragment multiplicities and the fragment charge correlations. The loss of memory of the entrance channel is an indication that equilibrium is attained prior to the fragmentation stage of the reaction. Besides the isospin, also the mass of the system play an important role for fragmentation observables of the reaction. From fig.3.8, we see the free nucleon increase with increase in energy for heavy nuclei while for light nuclei effect of energy almost independent of incident energy. To see the effect of symmetry energy on FN,

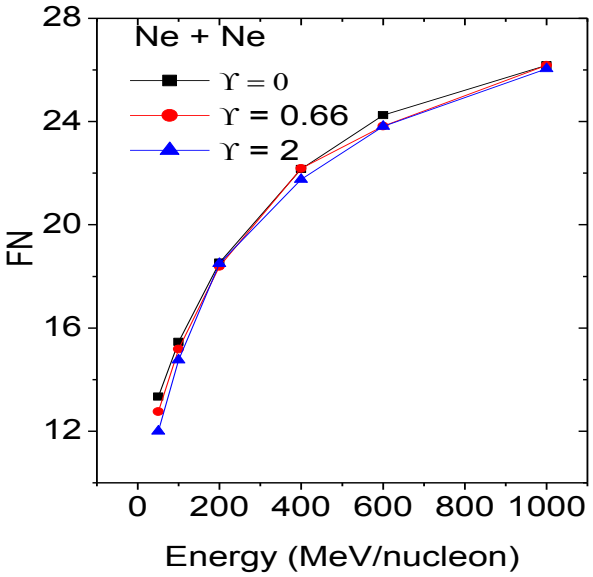

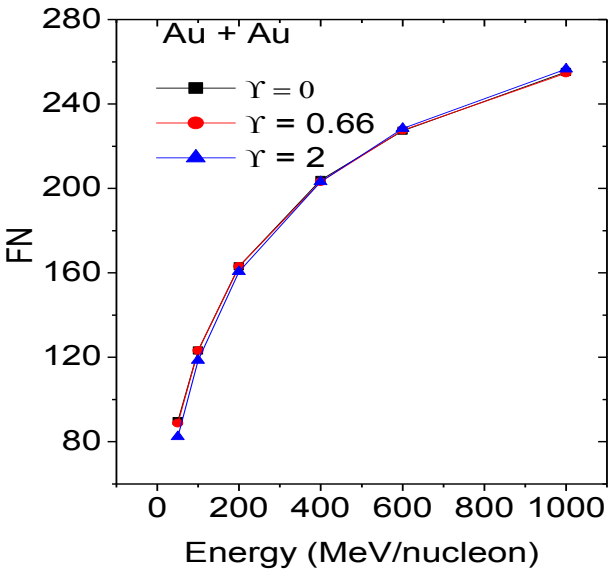

Fig. 3.8(a): Effect of incident energy on FN on colliding nuclei Ne + Ne at different ϒ values.

Fig. 3.8(b): Effect of incident energy on FN on colliding nuclei Au + Au at different ϒ values.

we plot FN production of Au + Au and Ne + Ne with respect to energy at different symmetry energy values. Fig. 3.8(a) and (b) represents the effect of ϒ density dependence of symmetry energy on colliding nuclei Ne + Ne and Au + Au at different incident energies. We analyse that for lighter nuclei in which neutrons and protons are equal in number shows different points for different ϒ at different energy. While for heavy nuclei Au + Au (neutron rich nuclei) ϒ = 0 and 0.66 give almost same point at all energies, but ϒ = 2 gives same result at high energy but vary at low energy.

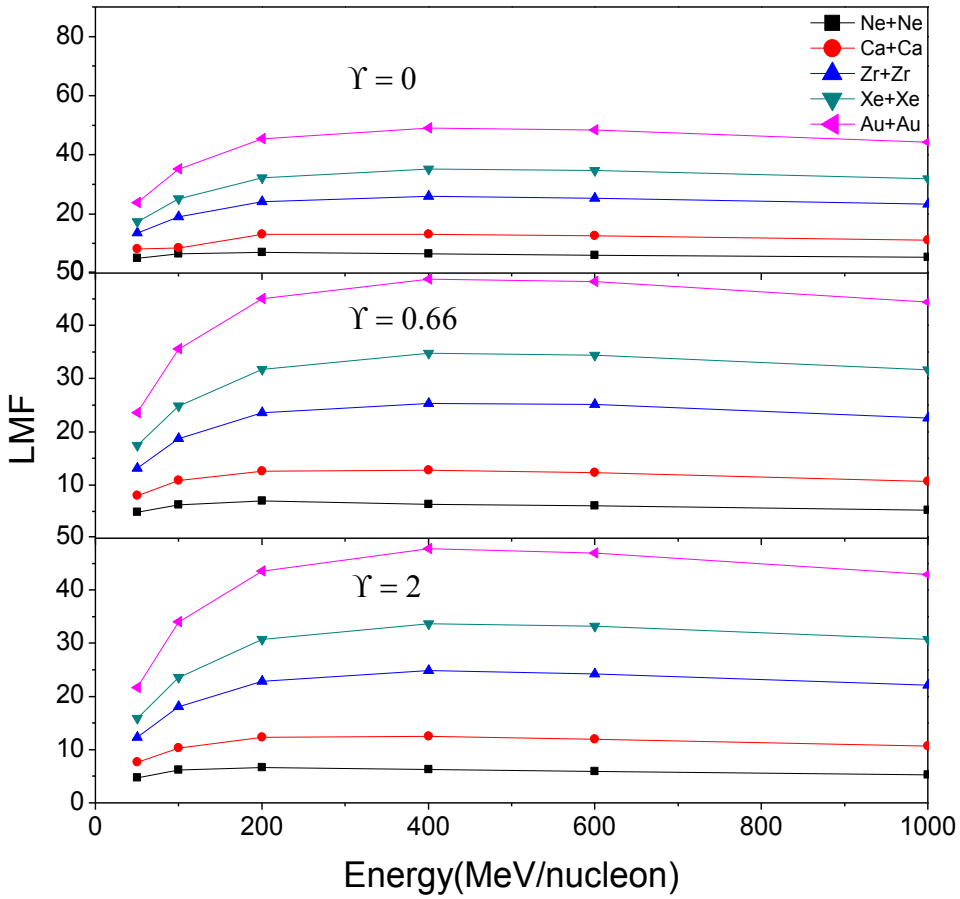

Fig. 3.9: Effect of incident energy on light mass fragments for different colliding nuclei.

On analysis the Fig.3.8-3.10 we observed that the number of fragment in FN>LMF>IMF. On considering the mass effect for lightest nuclei (Ne + Ne) at low energy (50 MeV/nucleon) the relative ratio of FN: LMF: IMF:: 8: 3: 1 and for high energy (1000 MeV/nucleon) is FN: LMF: IMF :: 7: 2: 1. The effect of incident energy is almost same from low energy to high energy for lighter nuclei, due less Coulomb effect. While for heaviest nuclei (Au+Au) at low energy relative ratio of formation of fragment is FN: LMF: IMF :: 9: 3: 1 and at high energy FN: LMF: IMF :: 83: 9: 1. There is large change in the formation of fragment, due to large compression at high energy and Coulomb repulsion. The effect of mass with incident energy is studied by A Schuttauf [13].

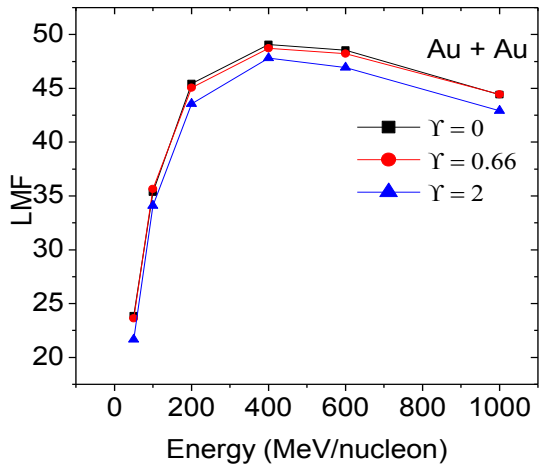

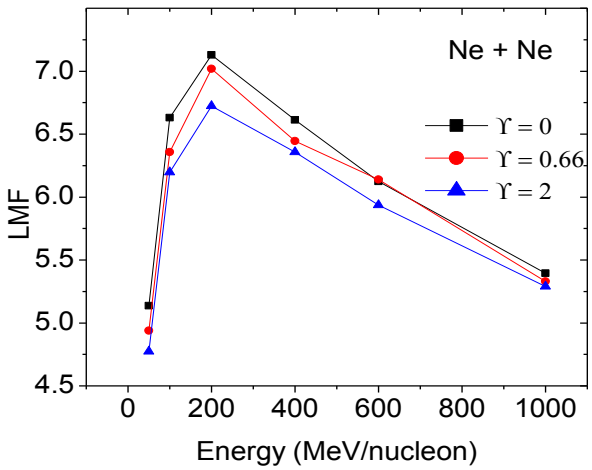

Fig. 3.9(a): Energy dependence on LMF of different symmetry energy of Au + Au nuclei.

Fig. 3.9(b): Energy dependence on LMF of different symmetry energy of Ne + Ne nuclei.

On analysis 3.9(a) and (b), we observed that influence of symmetry energy is more in LMF as compare to FN. In heavy nuclei effect of ϒ for values '0' and '0.66' is almost same while ϒ = 2 also shows same kind of output but at different points. From figure 3.9(b) one can observe the effect of symmetry energy on production of LMF's. So we can conclude from above two graphs that symmetry energy plays a vital role while study the LMF for light nuclei.

IMF production of heavy nuclei and light nuclei at different symmetry energy has been shown in fig.3.10. In heavy nuclei (Au +Au) symmetry energy shows its role only at low incident energy (50 MeV/nucleon) and for higher energies (100, 200, 400, 600, 1000) the effect decreases. On observing IMF's production for light nuclei we can say IMF increase with increase in the stiffness of symmetry energy as shown in figure 3.10(a) and 3.10(b).

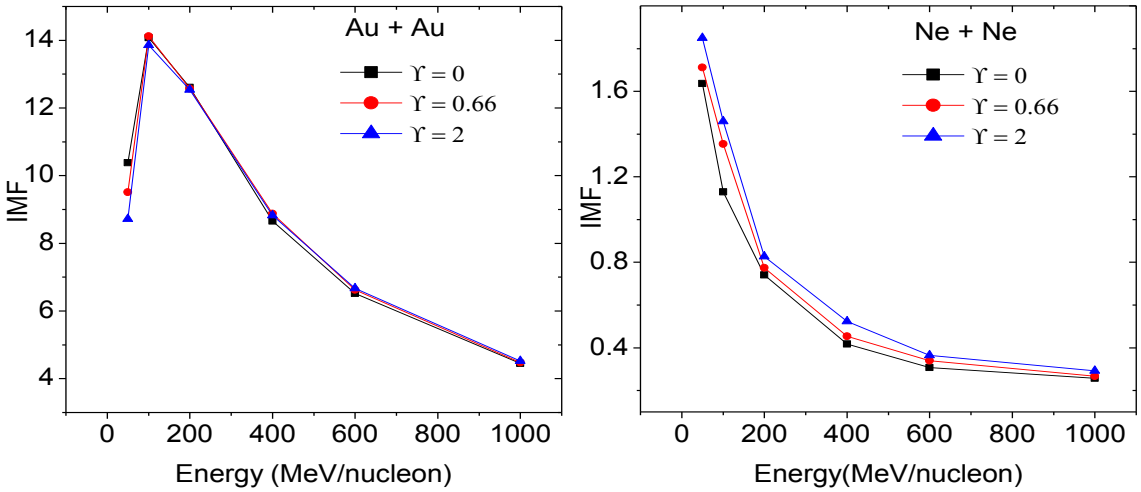

Fig. 3.10(a): Energy dependence on IMF of different symmetry energy of Au + Au nuclei.

Fig. 3.10(b): Energy dependence on IMF of different symmetry energy of Ne + Ne nuclei.

3.7 Cross-section

The nuclear cross-section is used to characterize the probability that a nuclear reaction will occur. The concept of a nuclear cross section can be quantified physically in terms of "characteristic area" where a larger area means a larger probability of interaction. Cross sections can be measured for all possible interaction processes together, in which case they are called total cross-section, or for specific processes, distinguishing elastic scattering and inelastic scattering amongst neutron cross-section the absorption cross-section are of particular interest.

3.7.1 Different nucleon-nucleon cross sections

Two nucleons can collide if they come closer than certain distance. The scattering of these nucleons is decided by a Monte Carlo procedure which is a stochastic scattering and hence is different from the Rutherford scattering. For nucleon-nucleon cross section σ, one can use a simple parameterization which depends on the centre of mass energy of nucleons [14]. In most of parameterizations of nucleon-nucleon cross-section, the following processes are always there:

$$N + N \rightarrow N + N \quad \text{(a)},$$
$$N + N \rightarrow N + \Delta \quad \text{(b)},$$
$$N + N \rightarrow \Delta + \Delta \quad \text{(c)},$$
$$N + \Delta \rightarrow N + N \quad \text{(d)},$$
$$\Delta \rightarrow N + \pi,$$
$$N + \Delta \rightarrow N + \Delta \quad \text{(e)},$$
$$\Delta + \Delta \rightarrow \Delta + \Delta \quad \text{(f)}.$$

(2)

In the literature, three type of cross sections, which are as

(a) Energy dependent [15]

(b) In-medium [16]

(c) constant cross sections [17]

We are interested in energy dependent and constant cross sections, so, in the following Sub-sections, they are discussed in detail.

3.7.2 Energy dependent nucleon-nucleon cross section

The energy dependent cross section is a parametric fit on the experimental data, which is derived by Cugnon et al.[15]. Here cross section is divided into elastic and inelastic parts which depend on the centre-of-mass energy available to the colliding pair of nucleons. For elastic channels, we use the total and differential cross section as [15]. These parameterized forms of the cross sections are in fact a fit to the experimental measurements. The limit of $\sqrt{s}$=1.8993 GeV is based on the fact that the mass of two nucleons is roughly equal to 1.876 GeV. Therefore, for two colliding nucleons with very small velocity, a constant cross section (= 55 mb) is used. The mass limit of the inelastic channel is based on the fact that mass of $\Delta(= N + \pi)$, is 1.076 GeV. Therefore, for $NN \rightarrow N\Delta$ channel, the outgoing mass should be at least 1.076+0.938 GeV. The graphical representation of the elastic and in-elastic parts of the cross section is displayed in fig.3.11. One sees clearly that the elastic cross section falls sharply in its initial stage and then saturate around 20 mb. Whereas, the in-elastic cross section starts increasing with increase in the bombarding energies. At very high energies, the nucleon-nucleon cross-section is fully dominated by the in-elastic channel. It is well known that the scattering cross section between two nucleons depends on their isospin.

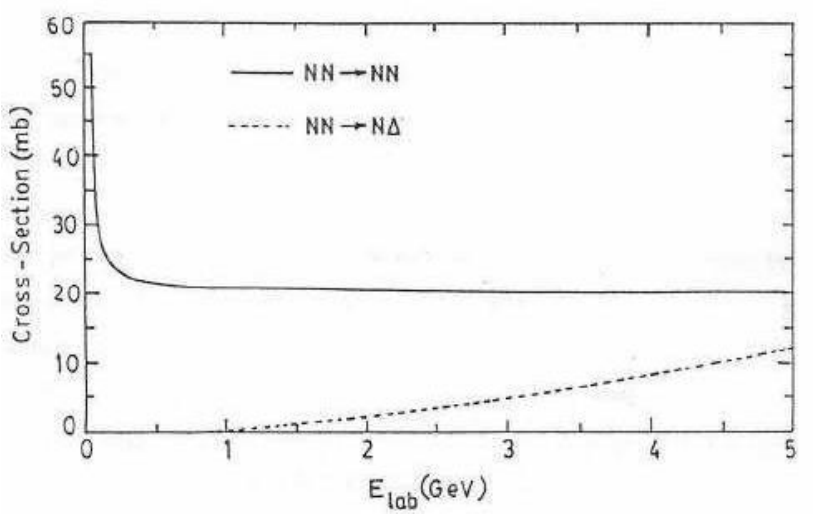

Fig. 3.11: The Cugnon parameterization for the elastic (solid line) and inelastic (dashed line) cross sections of nucleon-nucleon scattering as a function of the incident energy E_{lab}.

3.7.3 A constant nucleon-nucleon cross section

During early attempts, one has used a constant nucleon-nucleon cross section to study heavy-ion collisions through transport models. Several calculations based on a constant cross-section were applied to study the disappearance of flow and multifragmentation [17]. One has used isotropic and energy independent nucleon-nucleon cross sections with magnitude between 20 and 55 mb. It has also been shown by Zheng et al.[18] that a stiff equation of state with free nucleon-nucleon cross section and a soft equation of state with reduced cross section yield nearly the same results. Here we have used isospin independent cross-section to study the effect of multifragmentation. For comparison, we shall also use an isospin dependent cross-section. In figure 3.12 we see the effect cross-section on production of FN of two different multifragmentation reactions i.e. ratio of production of FN between a neutron rich nuclei Zr and a neutron deficient nuclei Ca under the effect of incident energy 50, 100, 200, 400, 600 MeV/nucleon at different symmetry energy. In first panel we consider isospin dependent cross-section. In second and third panel we use constant isospin independent cross-section with value 20 mb and 55 mb respectively. We can see that production in addition to symmetry energy is affected by different cross-section.

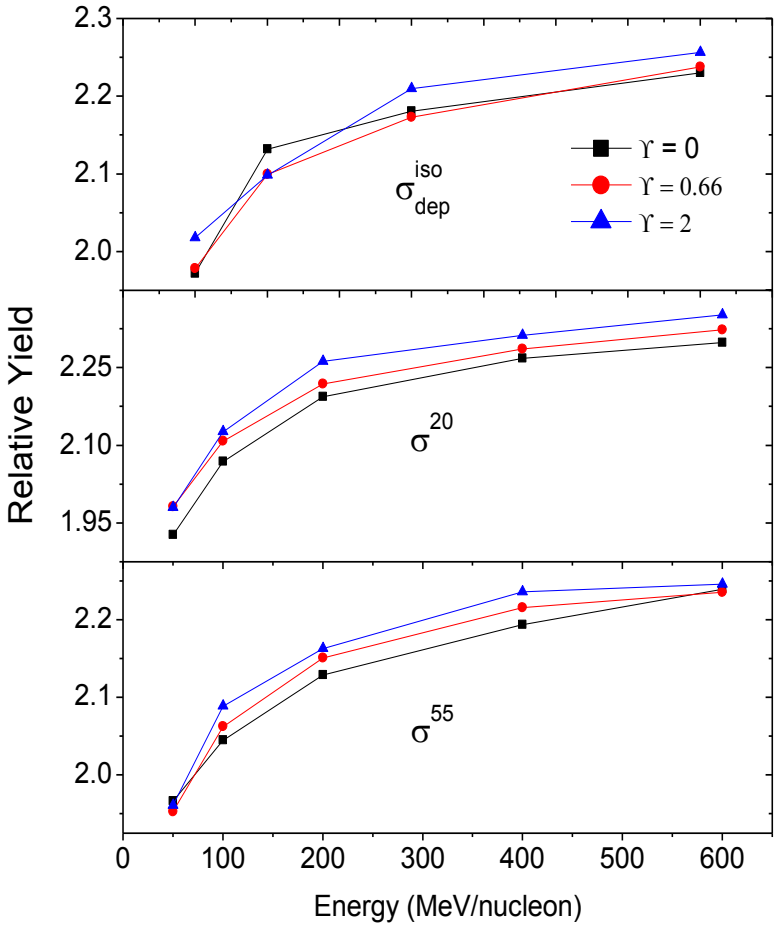

Fig. 3.12: Effect of cross-section with incident energy on production of free nucleon at different symmetry energy between a neutron rich nuclei Zr and neutron deficient nuclei Ca.

Similarly we can see the effect of cross-section on the production of LMF. We observe that the production of LMF increase as $\sigma^{55} < \sigma^{20} < \sigma^{\mathrm{iso}}_{\mathrm{dep}}$. Same effect is seeing in the production of IMF as shown in figure 3.14. We see that change in the production of FN, LMF, IMF is increase very fast up to energy 400 MeV/nucleon but change in production of fragments decrease at high energy i.e. above 400 MeV/nucleon.

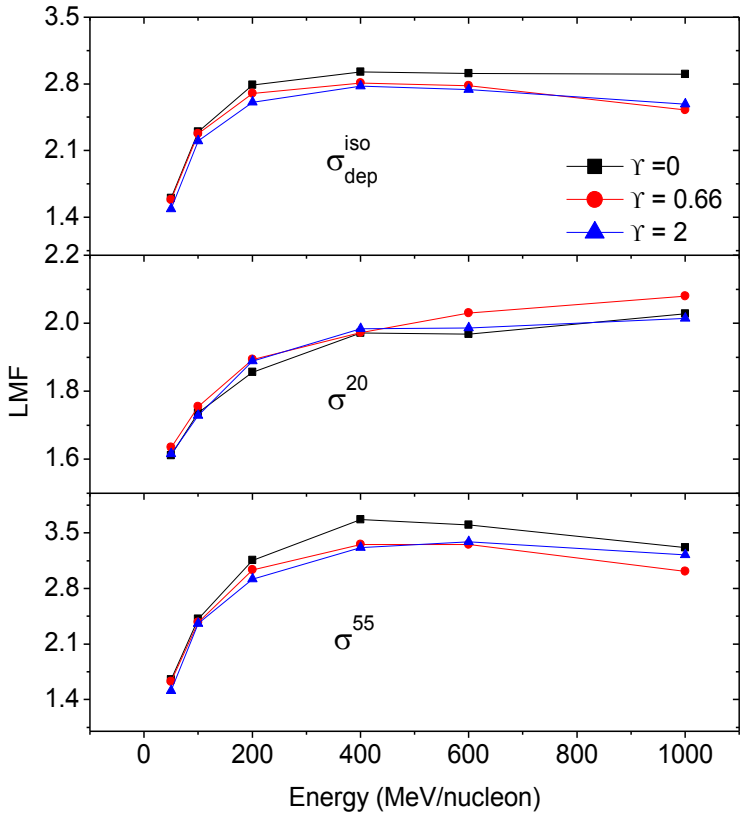

Fig. 3.13: Effect of cross-section with incident energy on production of light mass fragments at different symmetry energy between a neutron rich nuclei Zr and neutron deficient nuclei Ca.

The quantity Z_{bound} is defined as sum of all atomic charges Z_i of all fragments with Z> 2. Fig. 3.15 studies the multiplicity of IMF as a function of Z_{bound} for Zr + Zr nuclei at different cross-section. We see the effect of symmetry energy is almost negligible. IMF increase with increase the value of Z_{bound} due to the energy effect it decreases at high energy. Here we see the energy effect due to presence of neutron more than proton. While in case of $^{20}Ca_{10}$ + $^{20}Ca_{10}$ we have equal number of neutron and proton so IMF production increases with increase the value of energy. Also the property of rise and fall is missing in the IMF production for Zr + Zr reaction. Peak of fragment production is shifted in Zr + Zr, this fact has been verified in our recent studies [19].

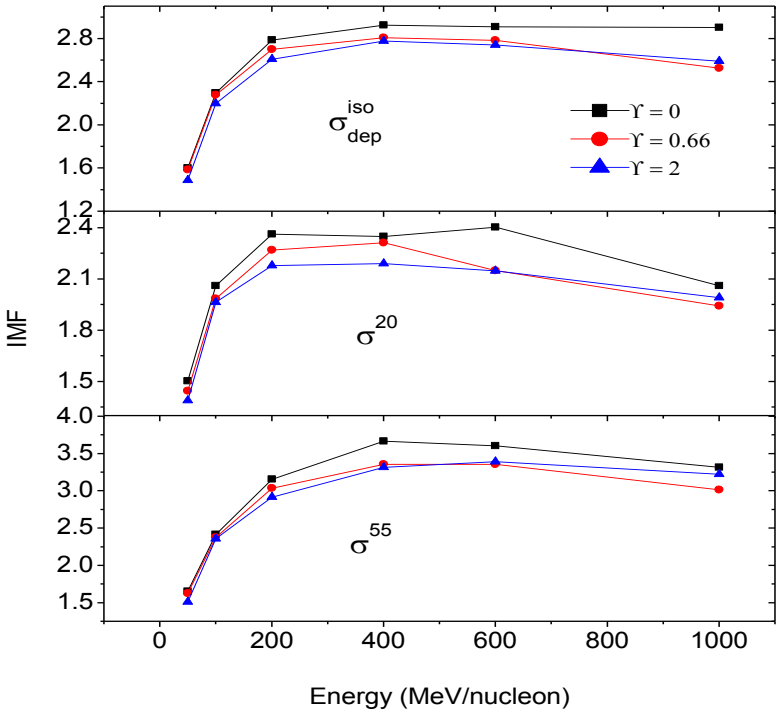

Fig. 3.14: Effect of cross-section with incident energy on production of intermediate mass fragments at different symmetry energy between a neutron rich nuclei Zr and neutron deficient nuclei Ca.

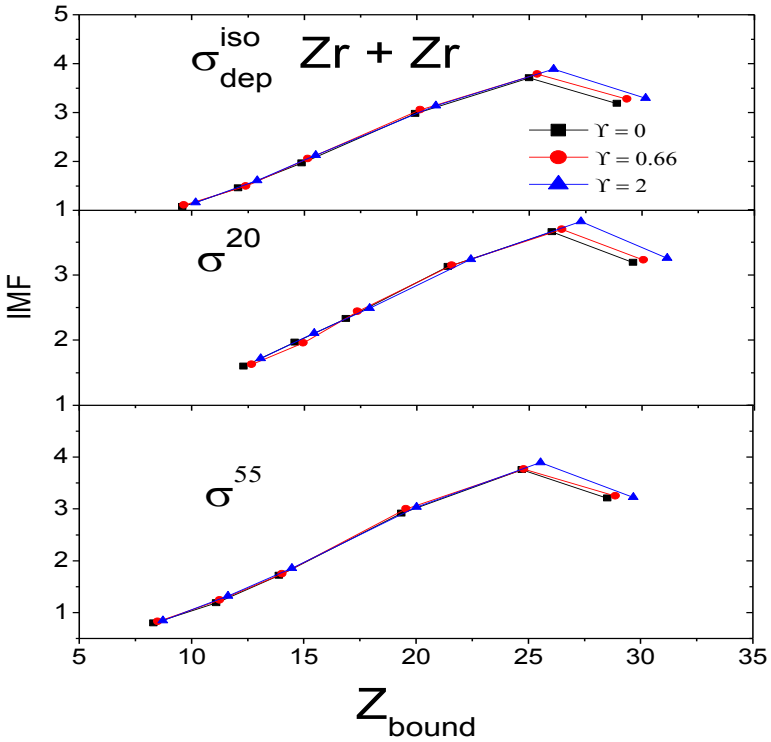

Fig. 3.15: Multiplicity of IMF as a function of Z_{bound} for Zr + Zr nuclei at different cross-section.

3.8 REFERENCES

[1] K. Sumiyoshi, H. Suzuki, and H. Toki, Astron. Astrophys. **303**, 475 (1995).

[2] R. R. Chasman, Phys. Lett. **B 577**, 47 (2003).

[3] J. Aichelin, Phys. Reports **202**, 233 (1991).

[4] A. Schuttauf et al., Nucl. Phys. **A 607**, 457 (1996); M. B. Tsang et al., Phys. Rev. Lett. **71**, 1502 (1993).

[5] T. Branz, L. S. Geng, and E. Oset, Phys. Rev. **D 81**, 054037 (2010); L. Tolos, A. Ramos, and E. Oset, Prog. Theo. Phys. Suppl. **168**, 635 (2007); E. Oset and H. Toki, Phys. Rev. **C 74**, 015207 (2006); A. Ramos and E. Oset, Nucl. Phys. **A 671**, 481 (2000).

[6] D. Gamermann and E. Oset, Phys. Rev. **D 80**, 014003 (2009).

[7] G. Peilert, H. Stocker, W. Greiner, A. Rosenhauer, A. Bohnet, and J. Aichelin, Phys. Rev. **C 39**, 1402 (1989); A. Bohnet, N. Ohtsuka, J. Aichelin, R. Linden, and A. Faessler, Nucl. Phys. **A 494**, 349 (1989); L. Neise, M. Berenguer, C. Hartnack, G. Peilert, H. Stocker and W. Greiner, Nucl. Phys. **A 519**, 375 (1990); M. Berenguer, C. Hartnack, G Peilert, H. Stocker, and W. Greiner, J. Phys. **G 18**, 655 (1992).

[8] B.de Schauenburg et.al., GSI Rep. No.98-1, 1997 (unpublished); G. S. Wang et.al.,ibid. 96-1, 1995 (unpublished.

[9] D. T. Khoa, N. Ohtsuka, A. Faessler, M. A. Martin, S. W. Huang, E. Lehmann, and Y. Lofty, Nucl. Phys. **A 542**, 671 (1992); D. T. Khoa, N. Ohtsuka, M. A. Matin, A. Faessler, S. W. Huang, E. Lehmann, and R. K. Puri, Nucl. Phys. **A 548**, 102 (1992); S. Kumar and R. K. Puri, Phys. Rev **C 58**, 320 (1998).

[10] Takuya Furuta and Akira Ono Phys Rev **C 79**, 014608 (2009). S. Kumar, S. Kumar and R. K. Puri, Phys. Rev. **C 78**, 064602 (2008).

[11] K S Vinayak and S Kumar, Phys. Rev. C, submitted (2011).

[12] E. Schiller, H. Muther, P. Czerski, Phys. Rev. **C 59**, 2934 (1999); P. Bozek, P. Czerski, Acta. Phys. Polo. **B 34**, 2759 (2003).

[13] A Schuttauf et al./Nuclear Physics **A 607** (1996).

[14] G. F. Bertsch and S. D. Gupta, Phys. Rep. **160**, 189 (1988).

[15] J. Cugnon, T. Mizutani, and J. Vandermeulen, Nucl. Phys. **A 352**, 505 (1981).

[16] A. Faessler, W. H. Dickhoff and M. Trefz, Nucl. Phys. **A 428**, 271c (1981).

[17] A. D. Sood and R. K. Puri, Phys. Rev. **C 70**, 034611 (2004); S. Kumar, M. K. Sharma, and R. K. Puri, ibid. **58**, 3494 (1998), A. D. Sood, R. K. Puri, and J. Aichelin, Phys. Lett. **B 594**, 260 (2004).

[18] G. Q. Li and R. Machleidt, Phys. Rev. **C 48**, 1702 (1993); T. Gaitanos, C.Fuchs, and H. H. Wolter, Prog. Part. Nucl. Phys. **53**, 45 (2004); Y. Zhang, Z. Li, and P. D anielewicz, Phys. Rev. **C 75**, 034615 (2007).

[19] V. Kaur and S. Kumar, Phys. Rev. **C 81,** 064610 (2010).

CHAPTER 4

Summary

The thesis contains a brief review of one of the important branch of nuclear physics i.e. heavy ion physics. The isospin dependent quantum molecular dynamics model (IQMD) is used to describe the effect energy and time evolution during the collision. It contains the theoretical study of density dependence of symmetry energy.

In chapter 2 history of model and isospin quantum molecular dynamics model is explained in detail. Then method of clusterization i.e. minimum spanning tree method is also discussed.

In chapter 3 we see effect of energy and time evolution on the production of different fragments. We also see the phase space, cross-section and mass dependence on different fragments i.e. on free nucleon, light mass fragments and intermediate mass fragments in detail.

Conclusions

1. Multiplicity is affected by energy and mass and to very small extent by different form of symmetry energy.
2. Symmetry energy almost independent for production of FN.
3. Production of LMF's and IMF's for light nuclei affected more by symmetry energy as compare to heavy nuclei.
4. Isospin dependent and isospin independent cross-section influence the production of fragments.

Influence of symmetry energy on fragment production

A dissertation submitted in the partial fulfilment of requirement for the award of the

Degree of

Masters of Science InPhysics

Submitted by
RUBINA BANSAL
Roll no.-300904013
Under the esteemed guidance of
Dr. Suneel Kumar
(Assistant professor)
School of physics and material science
Thapar University
PATIALA (PUNJAB)-147004
June 2011.

Dedicated

To

My FAMILY

CERTIFICATE

This is to certify that the dissertation entitled ' Influence of symmetry energy on fragment production' submitted by Rubina Bansal (Roll no. 300904013) of M.Sc(physics), Thapar University, Patiala, was carried out by her under my supervision. This work has not submitted this material for credit towards any other degree at Thapar University, Patiala or any other University.

Dr.Suneel Kumar
Assistant Professor
School of Material Science and Physics,
Thapar University,
Patiala.

Countersigned by:

Dr. O.P. Pandey
(Prof. & Head)
School of physics and Material Science,
Thapar University,
Patiala.

Dr. S.K. Mohapatra
Dean of academic Affairs
Thapar University,
Patiala.

ACKNOWLEDGEMENT

I owe my deepest gratitude to **Dr. Suneel Kumar**, *my worthy supervisor*, who has been an inspiration during my work. Without him, this work would not have been possible. I thank him for his patience and encouragement that carried me on through difficult times, and for his insights and suggestions that helped to shape my skills. I express my sincere thanks to him for his valuable guidance in carrying out work under his effective supervision, encouragement and cooperation. His visionary thoughts have influenced me greatly. His dynamical attitude has empowered me with zeal of energy to conquer the minor details of my research work.

I also thank **Dr. O. P. Pandey**, Professor and Head, School of Physics and Materials Science for his support and providing facilities. Special thanks are due to all my friends and the staffs specially PhDs scholar **Anupriya Jain** and **Karan Singh Vinayak** at the School of Physics and Material Sciences for providing me a friendly atmosphere and encouraging me throughout this work.

I am deeply thankful to my Family their moral support and patience has bared fruit through completion of this report.

Date: (**Rubina Bansal**)

Place: Thapar University, Roll No. 300904013

Patiala.

ABSTRACT

The present work deals with the theoretical study dealing with influence of density dependence of symmetry energy on multifragmentation and in heavy ion collision at intermediate energies. We present a complete systematic theoretical study of multifragmentation for mass symmetric colliding nuclei for heavy-ion reactions in the energy range between 50 MeV/nucleon and 1000 MeV/nucleon by using soft equations of state using isospin dependent quantum molecular dynamics (IQMD) model. We envision an interesting outcome for symmetric colliding nuclei small but clear signature influence of density dependence of symmetry energy on fragmentation can be seen. The effect of isospin dependent and constant cross section also has been studied.

TABLE OF CONTENTS

Chapter 1 – Introduction

Chapter 2 – Methodology

List of figures

Fig.3.8(a). Effect of incident energy on FN on colliding nuclei Ne + Ne at different ϒ values.

Fig.3.8(b). Effect of incident energy on FN on colliding nuclei Au + Au at different ϒ values.

Fig.3.9. Effect of incident energy on light mass fragments for different colliding nuclei.

Fig.3.9(a). Energy dependence on LMF of different symmetry energy of Au + Au nuclei.

Fig.3.9(b). Energy dependence on LMF of different symmetry energy of Ne + Ne nuclei.

Fig.3.10(a). Energy dependence on IMF of different symmetry energy of Au + Au nuclei.

Fig.3.10(b). Energy dependence on IMF of different symmetry energy of Ne + Ne nuclei.

Fig.3.11. *The Cugnon parameterization for the elastic and inelastic cross sections of nucleon-nucleon scattering as a function of the incident energy* $E_{lab.}$.

Fig.3.12. Effect of cross-section with incident energy on production of free nucleon at different symmetry energy between a neutron rich nuclei Zr and neutron deficient nuclei Ca.

Fig.3.13. Effect of cross-section with incident energy on production of light mass fragments at different symmetry energy between a neutron rich nuclei Zr and neutron deficient nuclei Ca.

Fig.3.14. Effect of cross-section with incident energy on production of intermediate mass fragments at different symmetry energy between a neutron rich nuclei Zr and neutron deficient nuclei Ca.

Fig.3.15. Multiplicity of IMF as a function of Z_{bound} for Zr + Zr nuclei at different cross-section.